

SOME PROBLEMS OF SHORT PULSE, LOW ENERGY, HIGH REPETITION RATE LASERS
APPLIED TO SATELLITE RANGING SYSTEMS *

R.L. Hyde and D.G. Whitehead,
University of Hull,
England

Introduction

It is generally accepted that to achieve a satisfactory photon return rate from satellite-borne reflectors, at an accuracy limited only by atmospheric uncertainties, sub-nanosecond, high peak power laser pulses are necessary. To provide adequate statistical data, a fast repetition rate is required, necessitating a high average power transmitter.

It is the purpose of this paper to outline the problems associated with such lasers and to suggest ways of overcoming them.

1. Laser Limitations

Solid state laser oscillators producing sub-nanosecond pulses are at present limited to around 20Hz repetition rate by thermal transients which disturb the fine balance within the optical resonator and high peak power non-linear effects which can lead to wavefront distortion and the irreversible breakdown of materials.

The effect of non-linear interaction with optical materials manifests itself as ⁽¹⁾

- (a) non-linear lensing,
- (b) small-scale self-focusing.

The physical process occurring is predominantly orbital electronic polarisation in the solid state.

* First presented to the 3rd Laser Workshop, Lagonissi, 1978 and revised in 1981.

The refractive index (n) of an optical material can be described thus:

$$n = n_0 + \frac{\mu_0 c}{n_0} \cdot n_2 I \quad \dots(1)$$

where n_0 is the linear refractive index and n_2 is a non-linear parameter, its term being dependent upon the beam intensity I. The intense part of the beam profile (usually the centre) traverses a marginally longer optical path, retarding the wavefront and causing the beam to converge. This is referred to as non-linear lensing, and may eventually result in very high intensities greater than the intrinsic dielectric breakdown strength of the material. We may define a critical power such that the natural diffraction is negated by this convergence. For a beam of Gaussian profile this is given by:

$$P_{\text{critical}} = \frac{1}{4\pi\mu_0 c} \cdot \frac{\lambda^2}{n_2} \quad \dots(2)$$

and is of the order of 600kw for Nd:YAG. The non-linear lensing focal length for a Gaussian beam is given by:

$$Z_f = \frac{2\pi}{\lambda} \cdot \omega^2 \cdot \left(\frac{P}{P_{\text{critical}}} - 1 \right)^{-1/2} \quad \dots(3)$$

where ω is the e^{-1} beam radius at the input. It is, of course, essential to ensure that Z_f is much greater than the extent of the laser optical system. As P varies within the pulse duration, Z_f will vary and limit a resonant cavity's stability.

When the power is much greater than the critical power the beam may break up into many parts. This is called small-scale self-focusing. The optical gain is a function of wavefront spatial frequency, and wavefront noise due to optical imperfection in the propagation path will be exacerbated. This can be controlled in an amplifier chain by periodically filtering the wavefront noise before it is established, and in an oscillator will tend to be dispersed by diffraction. In either case it is a limiting factor.

In addition to these fundamental limitations to the use of very high power pulsed lasers, the laser sub-system itself will be the least reliable component in a satellite laser ranging system. This is because of the finite life-time of components such as flashlamps, dielectric coatings and crystal optics. Its development is still at an early state compared to, for example, tracking telescopes, and its reliability cannot compete with silicon-chip based technology.

It makes design sense therefore, to use a minimal laser and where possible to assign the residual requirements of the satellite laser ranger elsewhere.

2. The Minimal Transmitter

This is a laser oscillator only, consisting of a single traverse mode low loss resonator, a means of producing optical gain, a resonant modulator for longitudinal mode-locking and a resonator Q-switch to inhibit premature oscillation. Several designs are in existence and their categories may be described as CW, quasi-CW, or pulsed, each with a stable or an unstable resonator and modulated actively or passively. Such a device has an output of bandwidth-limited pulses at a very stable repetition frequency. Single pulse duration may be a few picoseconds and can be lengthened by auxiliary etalons.

CW systems require extensive amplification to be useful in satellite laser ranging applications, and we shall direct our comments to Nd:YAG pulsed and quasi-CW systems, having repetition rates of the order of 10Hz and an average power of the order of 30mW. The fundamental wavelength is 1.06 μ m and the pulse duration as short as 25 picoseconds.

It is prudent to consider such a minimum performance/maximum reliability specification and ask if, and how, it may be used in a satellite laser ranging system. We first ask whether the receiver can accept a repetitive burst of pulses (pulse burst mode) and whether they can be successfully analysed. Operation may involve several bursts in flight at any one time, each burst

consisting of a comb of precisely spaced pulses. Secondly, we consider what satellites are accessible to such a laser transmitter. Finally we question the necessity for second harmonic operation.

3. Pulse Burst Mode

The use of a pulse burst presents no great problem for the receiver and timing electronics if the spatial separation of each pulse is constant and greater than the time precision to which the satellite range is already known. Under these conditions the precise comb pulse, from which the return signal originated, can readily be identified. Unfortunately, at present, such precise satellite range predictions are not available. However, providing, that sufficient returns can be obtained from a sequence of shots, decoding of the comb can be carried out statistically. For example, it can be shown that⁽²⁾ only some 15 returns are necessary to decode a comb to within 6 nanoseconds, the returning signals conserving the comb shape as they accumulate.

It should be noted that the transmission of a burst of accurately timed pulses creates the possibility, in favourable circumstances, of detecting photons for more than one pulse. However, multiple timers or some form of time store⁽³⁾ must be used, as the computing period of the verniers, necessary to achieve picosecond resolution⁽⁴⁾, is greater than the pulse separation. The probability of several returning photons being detected is small, but the difficulty of accurately locating the target would seem to indicate that there may be an advantage in being able to make use of two or more return signals following a successful target acquisition.

It is also desirable to be able to accept more than one signal when using single pulse ranging systems, thus preventing noise photons from invalidating a ranging shot. Subsequent analysis can then separate received noise photons (random epoch) from the true return.

4. Multiple Pulse Trains

The ability of the laser system to operate at relatively high repetition

rates, demands that the timing of pulse bursts be on an epoch basis, since several may be in flight at once. In practice, the number in flight will be limited by the necessity to shut down the laser when a return is expected, as the electrical noise generated by the laser would otherwise saturate a sensitive receiver. However, it is a relatively simple matter to control the firing of the laser, based on a prior knowledge of the target range.

5. Satellite Accessibility with a Minimal Transmitter

We define the Minimal Transmitter as a pulsed neodymium laser oscillator transmitting a comb of 3mJ at 10Hz (30mW).

It is necessary to determine the efficacy of such an emitter in ranging to, for example, LAGEOS.

1. The probability of a return ($\pi(R)$) must be greater than a $n/p.t$ where n is the number of returns in a bin 'necessary for recognition' and $p.t$ a specified number of shots;

$$\pi(R) > n(p.t)^{-1} \quad \dots(4)$$

2. Assuming Poissonian statistics the probability of a return is given by;-

$$\pi(R) = \exp(-\bar{n}_B) \{1 - \exp(-\bar{n}_S)\} \quad \dots(5)$$

where

$$\bar{n}_S = \left(\frac{E}{2\pi \cdot \Omega_1 \cdot h\nu}\right) (A_3 \cdot \epsilon_2 \cdot \eta) (S)^{-1} \quad \dots(6)$$

and

$$\bar{n}_B = \left(\frac{N(\lambda)}{h\nu}\right) (A_3 \cdot \epsilon_2 \cdot \eta \cdot \Omega_2 \cdot \Delta\lambda) t_g \quad \dots(7)$$

where the satellite-channel parameter

$$S(v, \alpha, \lambda) \equiv \frac{R^4}{a^2 \sigma} \text{ and } a^2 = \exp(-2\tau_t' \cdot \sec(90-\alpha))$$

Figs. 1 and 2 shows how S varies with α for certain met. conditions and two wavelengths $\lambda = 1.06\mu\text{m}$ and $\lambda = 0.55\mu\text{m}$ for LAGEOS. Values of τ_t' are shown in Table 1.

Combining equation 4 and 5 and taking the zero background case for an example.

i.e. when $\bar{n}_B \rightarrow$ zero. Then

$$p. \bar{n}_s \geq n/t. \quad \dots (8)$$

for a given system

$$\bar{n}_s \approx \frac{K_s}{S \cdot \Omega_1} \quad \dots (6a)$$

$$\therefore p. \frac{K_s}{S \cdot \Omega_1} \geq n/t \quad \dots (9)$$

Comparing the two cases of equation 9 for $\lambda = 1.06\mu\text{m}$ and $0.53\mu\text{m}$ we have

$$r \equiv \frac{K_{s.S^{-1}} (\lambda = 1.06)}{K_{s.S^{-1}} (\lambda = 0.53)} \quad \dots (10)$$

$$r = \frac{8}{30} \cdot \left[\frac{S(.53)}{S(1.06)} \right].$$

i.e. the break-even point for $\frac{S(.53)}{S(1.06)}$ is ≈ 4 .

This is plotted for LAGEOS in Fig. 3 where we see that the fundamental wavelength is preferable for low angles and visibilities. Returning to equation 9 and substituting some typical parameters

$$p = 10\text{Hz}$$

$$K_s = 1 \times 10^{11}. \quad (\lambda = 1.06\mu\text{m})$$

$$\frac{10^{12}}{S \Omega_1} \geq \frac{n}{t} \approx \frac{1}{10} \quad \dots (9a)$$

$$\text{i.e. } S \Omega_1 < 10^{13}. \quad \dots (11)$$

$$\text{now } S(5\text{km}, 20^\circ, 1.06, \text{LAGEOS}) \approx 10^{22} \text{ m}^2$$

i.e. a 30μ radians field of view is required, which is quite practical and realisable with current tracking telescopes.

6. Conclusions

This paper has identified some of the problems associated with the use of high power lasers for satellite ranging. It is pointed out that as the laser is inevitably the least reliable component in a ranging system, maximum system reliability can only be achieved by reducing the laser to its minimal configuration. The unique feature of the laser, the very high spectral radiance, and, in the case of mode-locked oscillators, a particular output format, should be utilised to the full. By transmitting a narrow beam in pulse burst mode at the fundamental wavelength, a greater degree of reliability is possible and techniques for accommodating such pulse trains can be readily applied to the detection and timing electronics.

7. Appendix I

n_o	Linear refractive index
n_2	Non-linear parameter
μ_o	Permeability of free space
c	Velocity of light
I	Intensity
λ	Wavelength
Z_f	Self-focusing distance
ω	$\frac{1}{e}$ Gaussian radius
P	Optical power
\bar{n}_s	Average signal return
\bar{n}_B	Average background return rate
$\eta(\lambda)$	Quantum counting efficiency
ϵ_2	Optical receiver efficiency
D	Telescope diameter ($A_3 = \frac{\pi}{4} D^2$)
E	Pulse energy
$h\nu$	Quantum energy
Ω_1	Full divergence solid angle
a	Atmospheric transmission
σ	Satellite cross-section
R	Satellite range
$N(\lambda)$	Background spectral radiance
Ω_2	Receiver field of view
$\Delta\lambda$	Receiver bandwidth
P	Repetition rate
t	Ranging period
t_g	Range gate
v	Meteorological range

8. References

1. 'Effect of Refractive Index Non-Linearity on the optical quality of High Power Laser Beams', B.R. Suydam, IEEE J. Quantum Electronics, Vol. QE-11, No. 6, June 1975.
2. Discussions with E.C. Silverberg, Lagonissi, May 1978
3. 'Multi-stop Timing Electronics for High Altitude Satellite Ranging', E.C. Silverberg, I.A. Malevich, Workshop on Laser Ranging Instrumentation, Lagonissi, 1978.
4. 'A Picosecond Timing System', M.J. Bowman, D.G. Whitehead, IEEE Trans. Inst. Meas., Vol. IM-26, No. 2, June, 1977.
5. Handbook of Geophysics and Space Environment, page 7-1, ed. S.L. Valley, (McGraw-Hill) 1965.

Table 1

λ (μm)	V	
	25km	5km
1.06	.14	.44
0.55	.36	.92

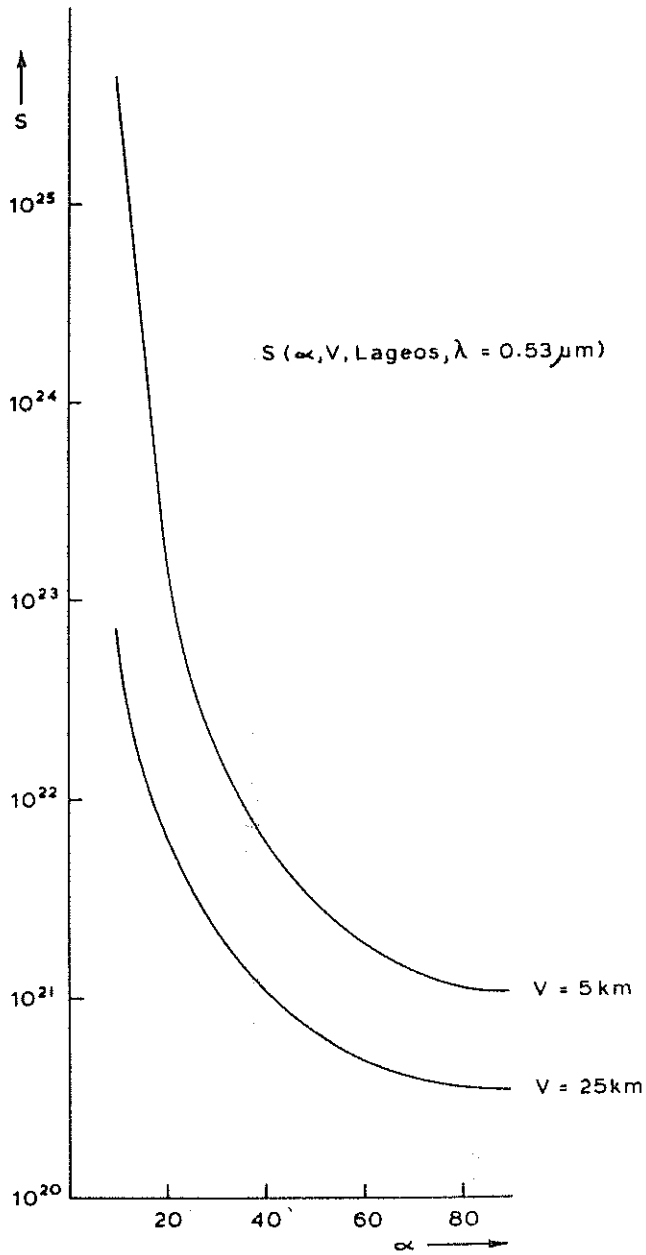


Fig. 1 Satellite - channel parameter S , versus angle of elevation α , with meteorological range as a parameter.

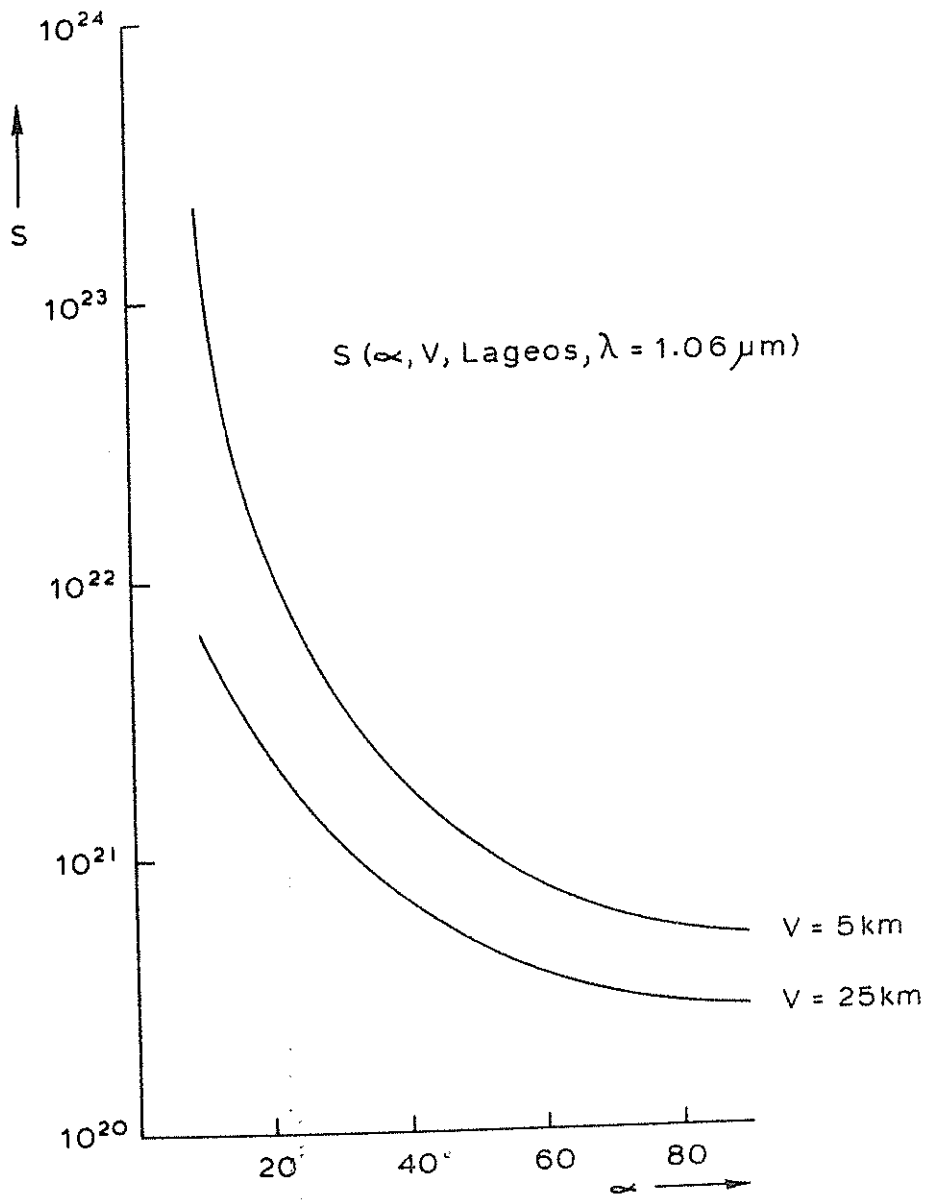


Fig. 2 Satellite - channel parameter S, versus angle of elevation α , with meteorological range as a parameter.

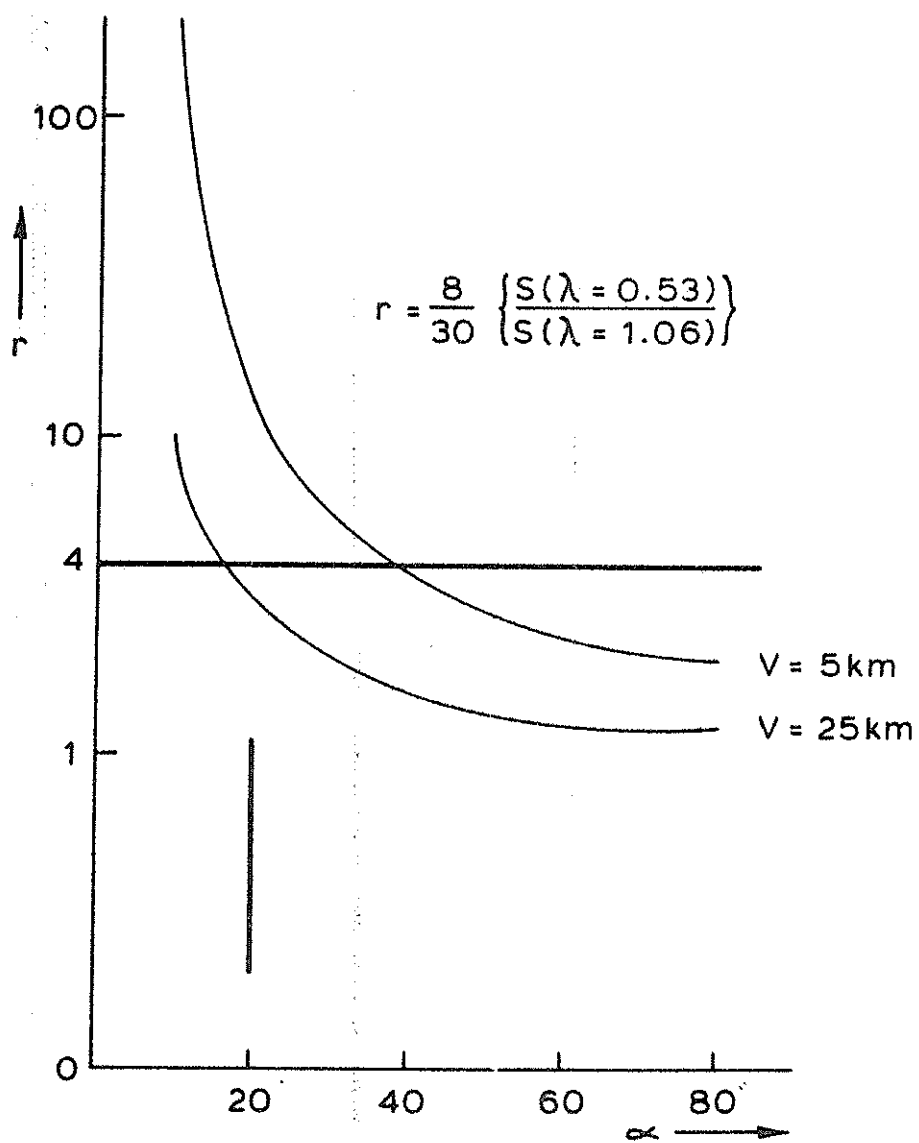


Fig. 3 The ratio of S for $\lambda = 1.06 \mu\text{m}$ and $\lambda = 0.53 \mu\text{m}$ against elevation angle with meteorological range as a parameter.

MODE-LOCKED Nd-LASER FOR THE UK SATELLITE LASER RANGING SYSTEM

C.L.M. Ireland, J.K. Lasers Ltd., Rugby, England

D.R. Hall and R.L. Hyde, Applied Physics Dept.,
Hull University, Hull, England

INTRODUCTION

The major Satellite Laser Ranging activity in the United Kingdom is funded by the Science and Engineering Research Council and is centred around a collaborative programme between the Royal Greenwich Observatory (RGO) and the University of Hull. The present objective of this programme is to design and build an SLR system to be sited within the RGO at Herstmonceux Castle in Sussex.

The design goal for this system is to attain the necessary performance to range to Lageos at 20° elevation from the sea level RGO site, to have both day-time and night-time capability and to achieve range resolution of a few centimetres. Satellite ranging measurements are scheduled to begin during 1982 to Lageos, Starlette and Geos C, and the station is planned to be fully operational for, and to participate in the next phase of the MERIT campaign.

This paper describes the mode-locked Neodymium:YAG laser which has been developed to meet the system requirement. The receiver sub-system and the aircraft detection/laser lockout sub-system are described elsewhere in the proceedings.

OVERALL LASER SYSTEM

The system design calculations indicated that the laser performance should meet the outline specification indicated below.

Wavelength = 532 nm
Pulse Energy \leq 30 mJ
Pulse Duration = 150 psec

PRF \leq 10 Hz
Life \geq 10^6 pulses free of service
Size, weight - minimal constraints for a static system

In addition, there are a number of extra features which it was felt necessary to incorporate into the design. These include built-in laser performance monitoring, eye safety precautions, beam processing optics and the provision of laser pulse timing signals. To achieve this performance a passively mode-locked Neodymium:YAG oscillator is used followed by two single pass amplifiers and a frequency doubler. A schematic diagram of the overall system is shown in Fig. 1. The laser optical system is mounted on a triple section optical rail two metres in length and 0.4 metres wide, and comprises, (a) a passively mode-locked and Q-switched Nd:YAG oscillator with a single pulse selector, (b) two optical single pass amplifiers, (c) a number of passive interstage optical components.

OSCILLATOR

The oscillator stage which occupies most of the right-hand side of the optical rail is shown schematically in Fig. 2. It comprises (A) a thin (0.25 mm) flowing dye cell contacted to a concave 100% reflecting rear cavity mirror, (B) a near field aperture, (C) a diamond pinhole, (D) an AR coated positive lens, (E) a $\frac{1}{4}$ " diameter x 3" long Neodymium:YAG crystal with wedged anti-parallel AR coated end faces in a single lamp pumping chamber fitted with optical corrector plates, (F) a temperature tuned output coupling etalon, (G) a single plate polariser in a vernier mount and (H) a single pulse selecting Pockels cell.

Since the peak output density can reach 2GWatt cm^{-2} , it is essential that the beam remain free of high spatial frequency noise as it propagates through the system. For this reason, the oscillator is designed to operate in the TEM_{00} fundamental mode and produce a near Gaussian spatial intensity distribution, free of any high frequency modulation. This beam profile is achieved in the oscillator by the use of an intracavity spatial filter and a near field aperture adjacent to the mode-locking dye cell.

Another common problem with this type of laser relates to the incidence of optical damage to the window of the dye cell. The first indication of such damage is an acoustic "tick" from the dye cell. If the laser is operated beyond this point, very weak sparks can be seen in the cell after a further $\sim 10^4$ shots, and typically the mode-locking reliability drops to about 50% after another $\sim 3 \times 10^4$ shots. A large number of measurements have been made in monitoring and studying this problem and it is now clear that (a) there is a fairly sharp threshold value of energy density on the cell window above which damage is a near certainty after 50-100 thousand shots, (b) the effect is cumulative in that the energy density threshold is 2-3 orders of magnitude below the published single shot data for fused silica or BK7 glass. In this system, the dye cell damage problem has been addressed by careful attention to cavity optical design and dye cell geometry and flow, and the use of single pulse selector-cavity dump in the oscillator design. The latter is achieved by inserting the Pockels cell switch inside the cavity and configuring the single pulse selector unit such that it not only selects a single pulse for subsequent amplification and doubling but also cavity dumps the oscillator so terminating all subsequent laser action. The details of this scheme can be understood by reference to Fig. 2. The single pulse selector is triggered by an early pulse in the train. Subsequently, a voltage step is generated in the switchout unit and propagates along a single transmission line to the Pockels cell switch. When the amplitude of this step is equal to the quarter wave voltage of the Pockels cell, light making a double pass through the cell has its plane of polarisation changed by 90° . Consequently, the pulse energy being fed back into the oscillator by the output etalon (F) is totally rejected at the intercavity polariser (G). The pulse energy being coupled out of the oscillator by the output etalon (F) makes a single pass through the Pockels cell and so is circularly polarised. At the subsequent polariser I, half the energy is transmitted and coupled into the rest of the system, and half is rejected. By this technique, the energy density incident on the damage sensitive mode-locking dye cell can be reduced by a factor of between 2 and 3.

AMPLIFIERS AND DOUBLER

The pulse produced by the oscillator passes through an in-line energy monitor which is coupled via suitable electronics to the computer, so that shot by shot monitoring of the oscillator performance can be logged. A pair of 45° mirrors are used to couple the beam into the other outer section of the rail and into a beam expanding telescope which precedes the first amplifier. Each amplifier contains a $\frac{1}{4}$ " diameter x 4" long Nd:YAG crystal which has wedged anti-parallel AR coated end faces in a single lamp pumping chamber in which the lamp and rod are surrounded by a close-coupling diffuse ceramic reflector. The two amplifiers are separated by a Faraday isolator, comprising a 55mm x 12mm high concentration terbium oxide glass rod (Hoya FR5) in a pulsed magnetic field positioned between a pair of single plate dielectric polarisers, which are set at 45° with respect to each other to yield high forward transmission while blocking any retro-reflection and inhibiting any possible oscillation between the two amplifier stages.

To produce frequency doubled output, a type II KD*P crystal, mounted in a temperature controlled oven is used to obtain critical phase matching. The doubler is followed by a pair of dichroic mirrors which are arranged to reflect the 532nm green component into the centre section of the rail. The beam then passes through a second in-line energy monitor and another beam expanding telescope before exiting into the Coudé system of the main tracking telescope. The 1060 nm infrared beam is used to trigger a fast timing photodiode positioned as shown in Fig. 1.

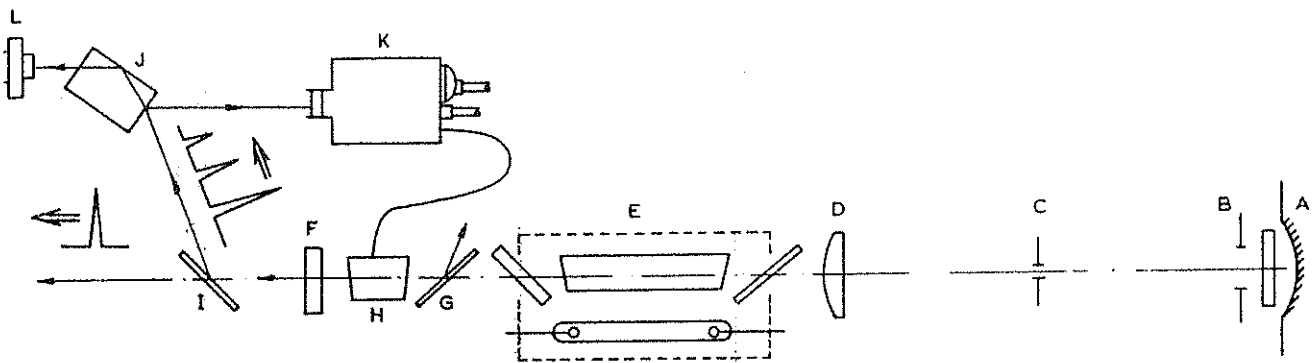
EYE SAFETY PRECAUTIONS

Since the ranging site at RGO is close to London's Gatwick Airport, a system is required to detect aircraft near the beam and subsequently inhibit laser output. The X-band radar detection system, which is described elsewhere in the proceedings, will produce a signal in the event that an aircraft is detected in the danger zone and this signal is used to close an electro-mechanical shutter positioned in the optical train within the oscillator. It has a closing time of less than 10 milli-seconds. A second, two position, shutter is situated near the output of the laser system (Fig. 1).

Aside from the open (100% transmitting) position, there is a second position in which a neutral density filter is inserted in the beam. This is selected so that after subsequent beam expansion the beam emanating from the telescope is eye safe.

LASER PERFORMANCE

The laser system described here produces an output energy of 30mJ per pulse at 532 nm at pulse repetition frequencies up to 10Hz. The duration has been measured with a streak camera at 150 ± 20 psec, corresponding to a peak power of 200 MW and an average power of 300 MW. The precautions taken with the oscillator have resulted in the possibility of uninterrupted operation for well over 10^6 shots and with a mode-locking drop-out rate of about 1/3000 measured at a prf of 10Hz. A photograph of the complete system is shown in Fig. 3.



- KEY**
- | | |
|---|--|
| A. Contacted dye cell with flowing dye.
Rear cavity 50cms radius, window
1/2° spectroslit wedge | G. Dielectric polariser |
| B. Near field aperture | H. Pockells cell with wedged windows and
crystal |
| C. SF pinhole | I. Dielectric polariser (crossed with G) |
| D. Recollimating lens | J. Beam steering glass block |
| E. Pumping chamber with 3" x 1/4" dia. YAG
rod and corrector plates | K. Photodiode triggered SPS unit generating
quarter wave voltage step |
| F. LaSF11 etalon | L. Fast photodiode monitor |

Schematic of mode-locked oscillator and SPS layout

Fig. 1 Oscillator Configuration

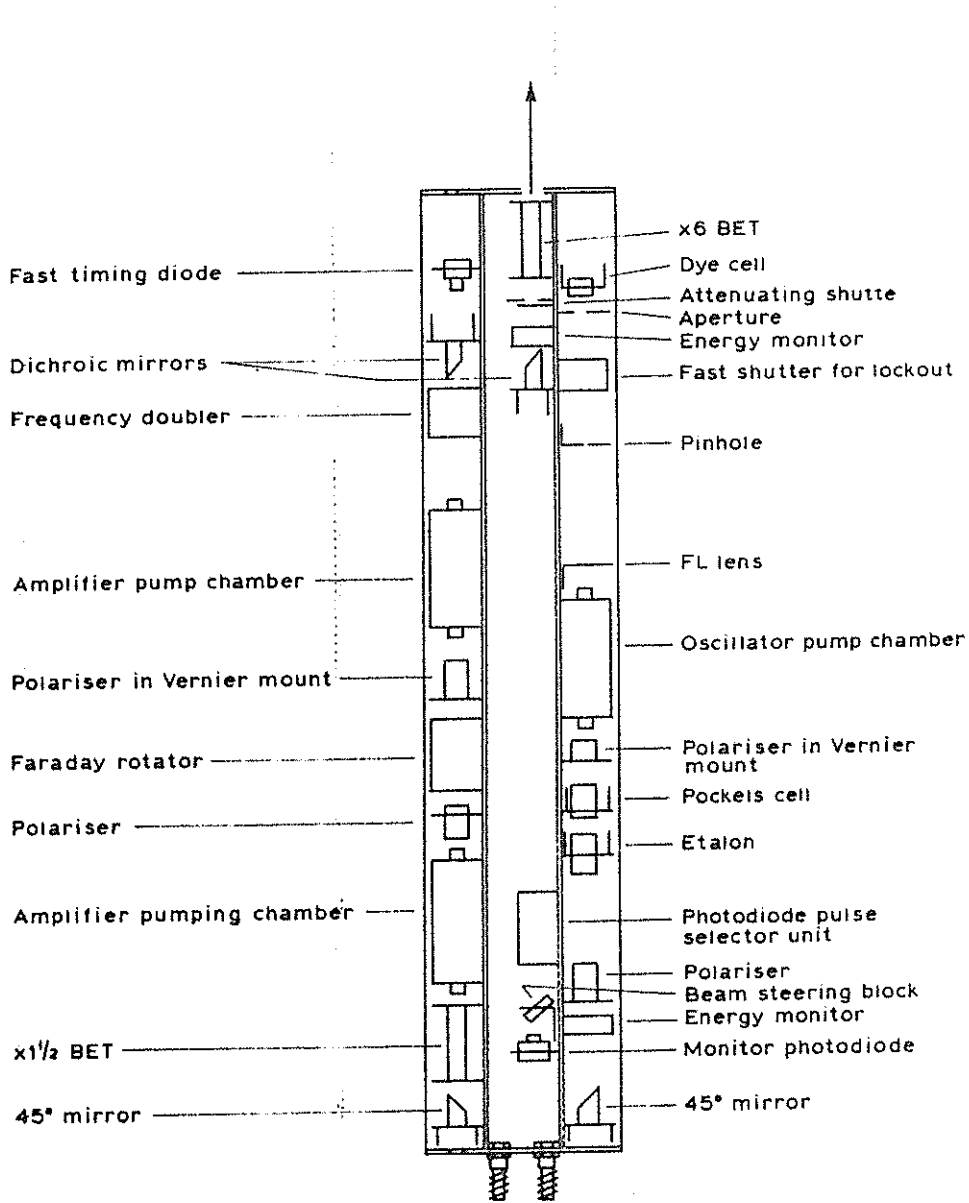


Fig. 2 Component Layout Schematic

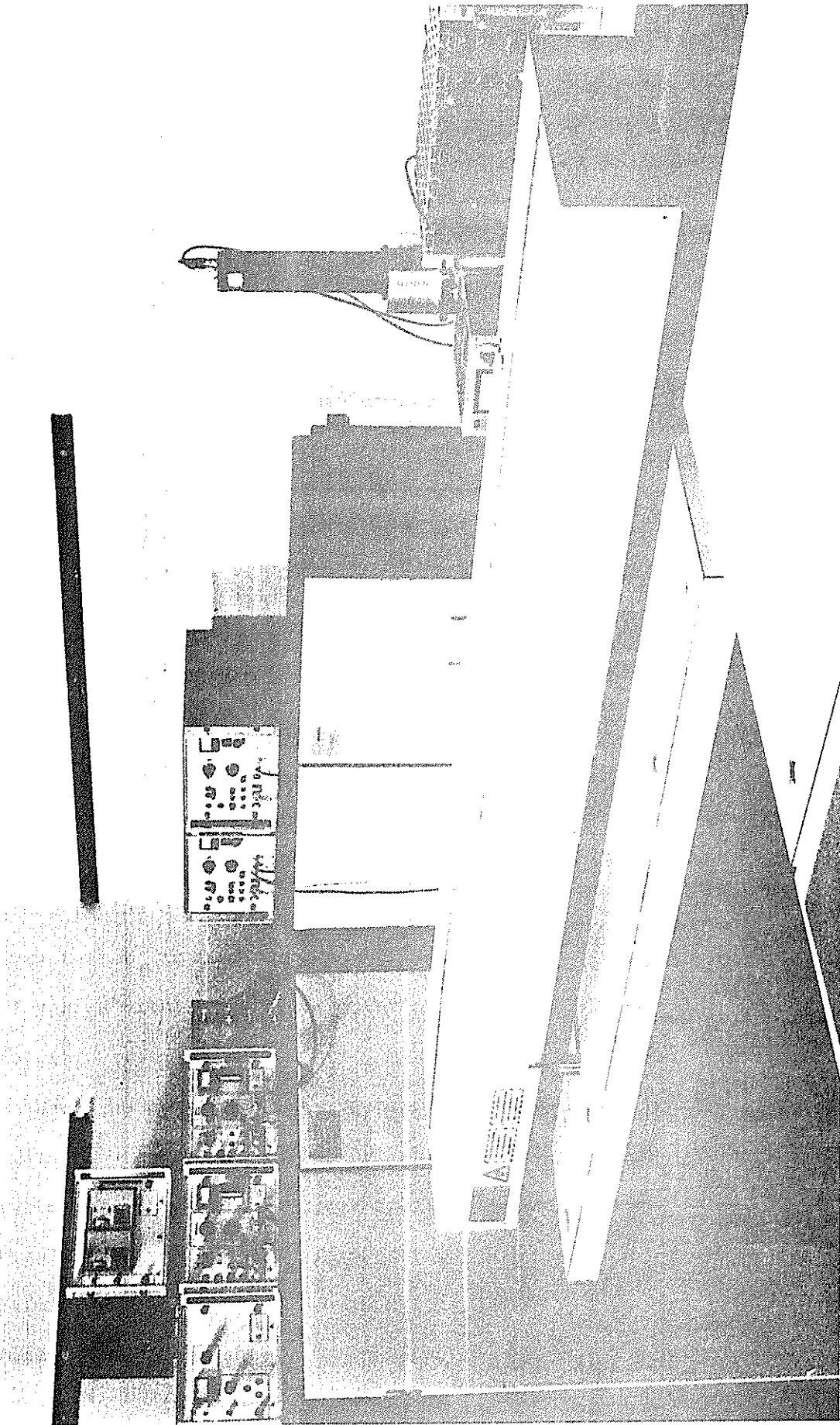


Fig. 3 Complete Laser System

CONSTANT GAIN PULSE FORMING LASER

H. Jelinkova

INTERKOSMOS

Faculty of Nuclear Science and Physical Engineering
Czech Technical University
Brehova 7, 11519 Prague 1
Czechoslovakia

There is a very strong interest to achieve a stable Q-switched output for any pulse laser application. For some of them, a pulse in nanosecond region, is desired. This report shows that both requirements are achievable using constant gain Q-switching plus pulse forming mode technique. The system has been applied for 2. generation laser radar.

CONSTANT GAIN REGIME

The long term instability (for example due to the lifetime of the flashlamp, cooling system dirty, blinding of pumping cavity surface, changing of coolant temperature, resonator distortion) results in a monotone change, usually, toward lower output energy and longer evolution time of the pulse. The short term instability (power supply voltage fluctuations, flashlamp output fluctuations due to the plasma formation instabilities, resonator distortion) results again in peak power and evolution time fluctuations from pulse to pulse.

To decrease the long and short term instabilities, instead of constant time, Q-switching at constant gain was implemented to Nd:YAG [1] and the ruby laser [2],[3]. The peak power, evolution time and the length of the pulse are strongly dependent [3],[4],[5] on the starting gain, which is function of the total fluorescence emission from the lasing medium. Thus, monitoring this fluorescence (Fig.1) with a photodiode, we obtain a signal indicating the gain function. This signal is compared to a stable reference voltage and it is independent of the total flashlamp output. The laser is Q-switched when its gain has decayed to a fixed trigger level (Fig.2). The flashlamp variations are accommodated by variation of the Q-switch time. The laser output should be, in absence of optical resonator distortion, constant.

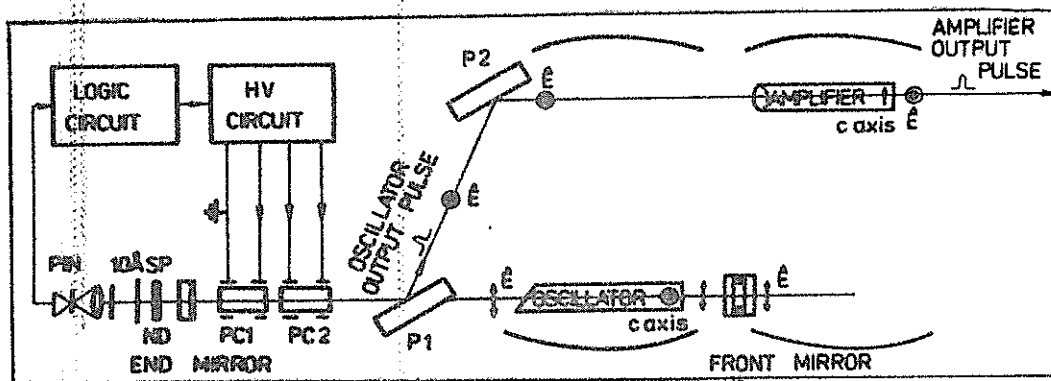


Fig.1 The principal scheme

To proof the stabilization when the laser is Q-switched at constant gain, we have set the desired gain via the reference voltage and we have changed the pumping energy from 1800 to 2400 J to simulate the instabilities. The stabilization of the output energy and the evolution time in dependence on input energy are shown on Fig.3 and Fig.4 resp. The stabilization, when the coolant temperature is changed, is shown on Fig.5.

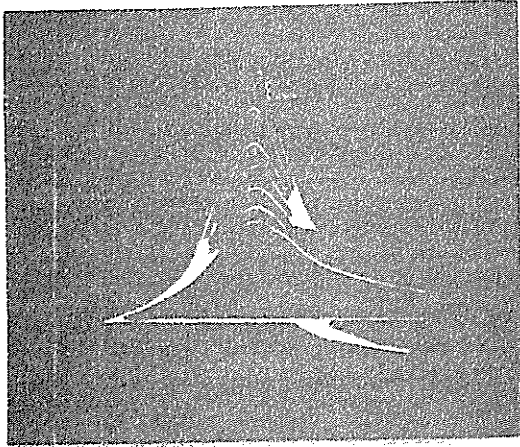


Fig.2 Ruby fluorescence versus time. The laser is pumped at different level and Q-switched at constant gain

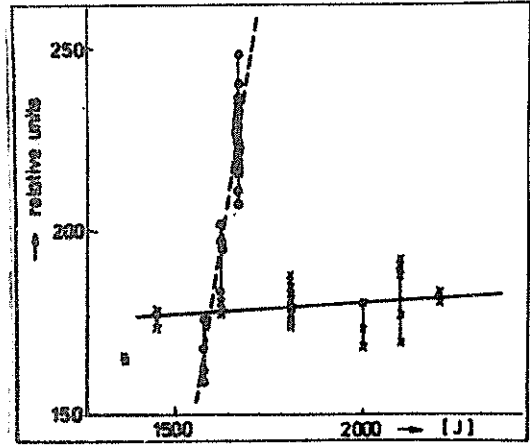


Fig.3 Output energy versus pumping. Dashed line \sim constant time, solid line \sim constant gain Q-switching resp.

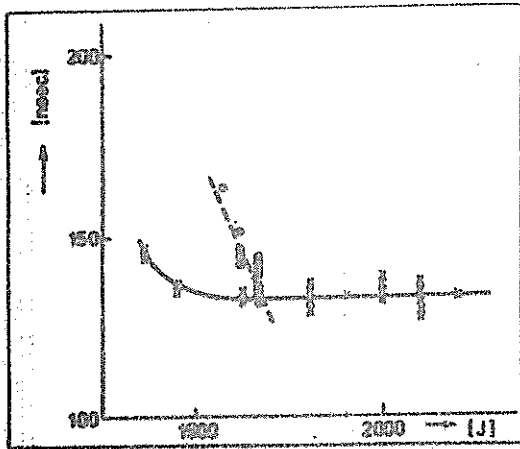


Fig.4 Evolution time of the pulse versus pumping. Dashed line \sim constant time, solid line \sim constant gain Q-switching resp.

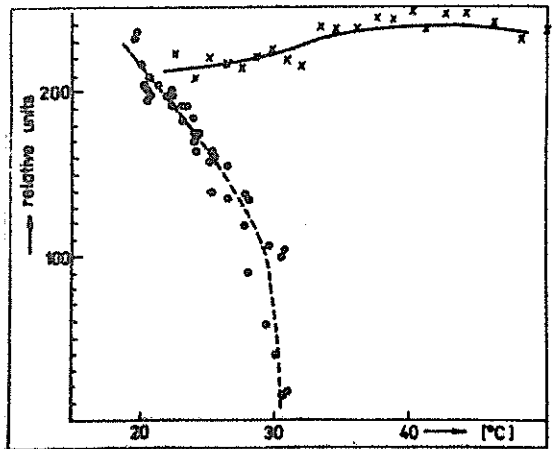


Fig.5 Output energy versus ruby coolant temperature. Dashed line \sim constant time, solid line \sim constant gain Q-switching resp.

THE PULSE FORMING MODE OR PTM MODE OF OPERATION

The implementation of constant gain Q-switching circuit into a ruby laser gave the possibility to use PTM mode [4] or the pulse forming mode (PFM) of operation with constant time delay. In our scheme (Fig.6), two krytrons are used for Q-switching and pulse forming of the laser pulse.

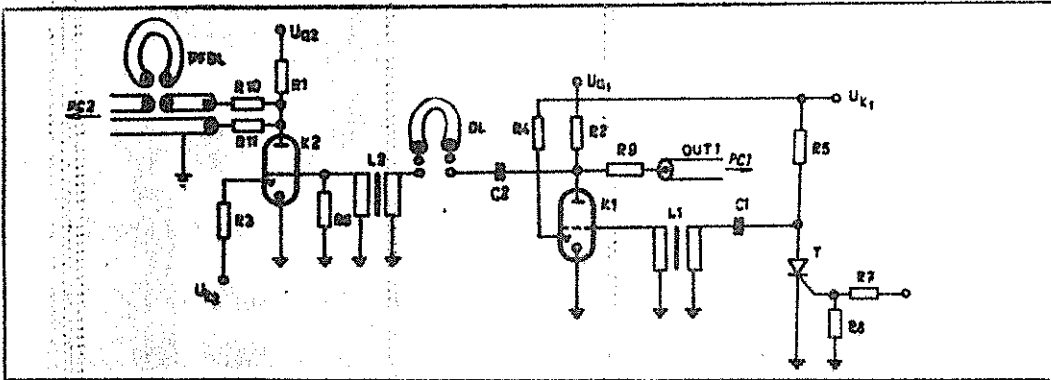


Fig.6 High voltage Q-switch and pulse forming circuit

The resonator is formed by the 90% plano dielectric mirror and the double plate crystalline quartz (or 80%) front mirror. As the active medium, 150x10 mm ruby rod cut perpendicular and 1° resp., is used. Between the rear mirror and 1° ruby end the Q-switching plus pulse forming assembly, consisting of the thin film dielectric polarizer P1 and two Pockels cells PC1, PC2, is placed. 10% of light, going through the rear mirror, passing the neutral density filters ND, polarizer SP and 10 \AA interference filter, is focused to the PIN photodiode. After the time delay (given by the cable DL) equal to the evolution time of the Q-switch pulse, the krytron K2 is switched. This voltage step pulse removes $\lambda/4$ voltage from one electrode of the Pockels cell PC2, thus re-introducing $\lambda/4$ relative phase shift to the passing light. It leads to rapid dumping of the opti-

cal energy from the cavity. After the time delay, from 1 to 5 nsec, given by the cable PFDL, zero voltage is on both electrodes of the Pockels cell PC2. The PFM pulse was generated. Using a longer cable than the laser cavity round trip, one obtains PTM operation. Records of resulted pulses are shown on Fig.7. Considering the rise time of our detection chain 1.8 nsec, the actual rise time of the output pulse is less than 2 nsec, the value typical for krytron KN 22B.

To amplify the output pulse, the polarizer P2 reflects the beam to the amplifier (Fig.1), the output energy is 0.1 - 0.2 J/nsec.

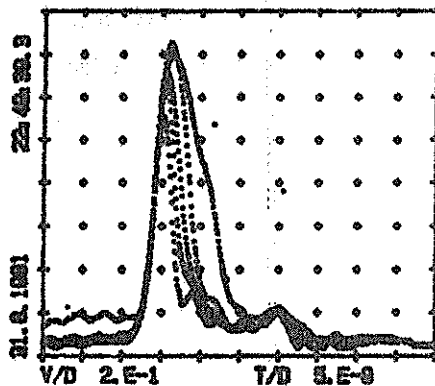


Fig.7 The output pulses

Consequently:

7 nsec	}	PTM regime
5 nsec		
4 nsec	}	PFM regime
3 nsec		
2 nsec		

CONCLUSION

The constant gain pulse forming technique gives the possibility to generate stable short nanosecond pulses. In principle, using a fast spark gap [6], [7], instead of krytron, this technique is one of the possibilities to obtain subnanosecond pulses.

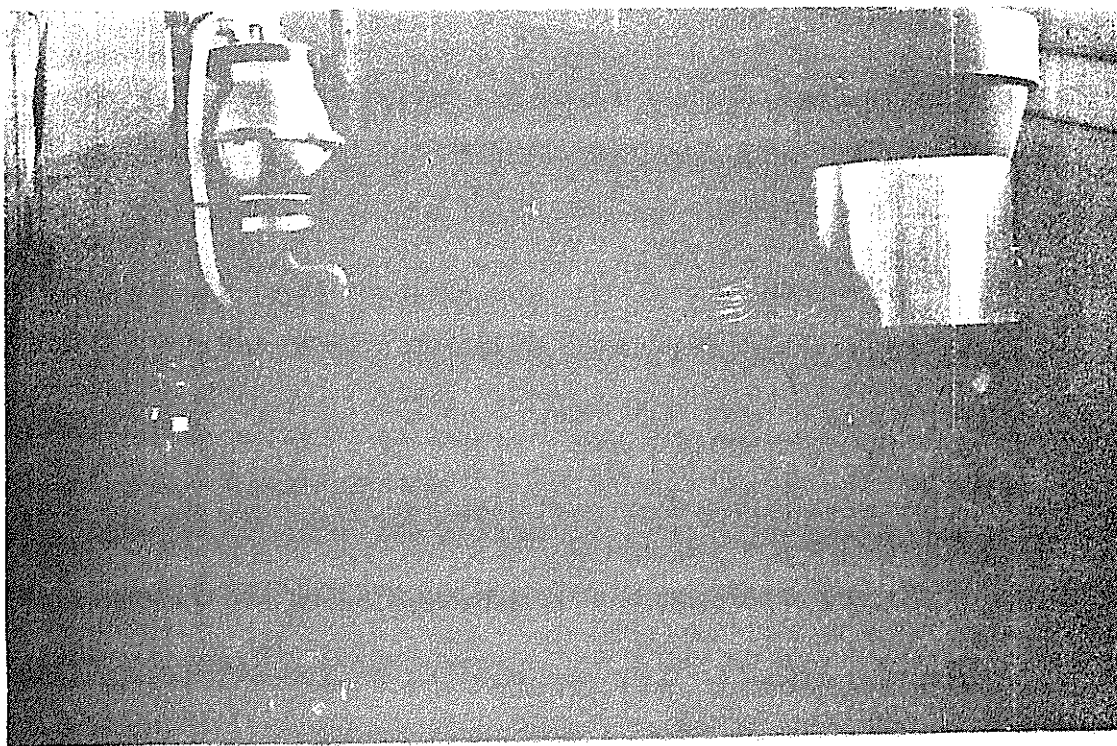


Fig.8 The photograph of the laser on the mount

REFERENCES

- [1] Downs D.C., Murray J.E., Lowdermilk W.H., IEEE Journal of Quantum Electronics, vol.QE-14, No.8, August 1978, P.571-573
- [2] Hamal K., Jelinkova H., Krajicek V., Novotný A., FJFI internal reports No.79/91, No.79/92, Prague 1979
- [3] Jelinkova H., to be published
- [4] Koehner W., Solid-State Laser Engineering, Springer-Verlag, New York 1976
- [5] Jelinkova H., PhD theses, Prague 1975
- [6] Jelinkova H., Hamal K., IEEE Journal of Quantum Electronics, vol.QE-14, No.10, October 1978, p.701
- [7] Krajicek V., Hamal K., Kubecek V., Schmidberger P., Proceedings of the 14th International Congress on High Speed Photography and Photonics, Moscow, USSR, October 1980, p.164

SUBNANOSECOND LASER SYSTEMS
FOR SATELLITE RANGING

H. PUELL

KRISTALLOPTIK LASERBAU GMBH
AM SULZBOGEN 62
8080 FÜRSTENFELDBRUCK, GERMANY

INTRODUCTION

There is evidently great interest in pushing the accuracy for satellite ranging down to several centimetres or less. This implies the use of a new laser generation, operating in the subnanosecond domain. Pulse durations of this order may be achieved by two different methods:

- i) mode-locking the laser oscillator, giving rise to a train of short light pulses equidistant in time, from which a single pulse may be selected and amplified further on. This method is readily employed with Nd:YAG lasers, generating light pulses as short as 30 psec.
- ii) pulse-slicing the output of a conventional Q-switched laser oscillator by means of a fast electro-optical shutter. This method is usually employed in case of ruby lasers, which generally show a very unstable mode-locking operation. Typical pulse durations of the order of 1 nsec are achieved by this method.

In this paper we wish to present examples for each of these methods. First we will describe the actively mode-locked Nd:YAlO₃ laser system,

which will be part of the Dutch-German Mobile Laser Ranging System (MLRS) built by the Technisch Physische Dienst (TPD), The Netherlands. In the second part, the performance of a special pulse-sliced ruby laser system, which was built for the station at Wettzell, Germany, will be discussed.

ND:YA10₃ LASER SYSTEM

The specifications of this laser system are shown in Tab.1. They result from the demands for high accuracy in ranging (pulse width), a large signal to noise ratio (output energy and repetition rate), and optimum adaption to the telescope and the detector (wavelength stability and bandwidth). Further boundary conditions concerning the power consumption, dimensions, and weight result from the mobility and the environment of the MLRS.

Wavelength	539 nm	Pulse width	200 - 300 psec
Stability	0.06 nm	Repetition rate	1, 2, 5, 10 Hz
Bandwidth	0.03 nm	Total weight	100 kp
Divergence	2 mrad	Dimensions	
Output energy	10 mJ	Power supply	100 x 35 x 60 cm
Stability	± 15 %	Optical bench	100 x 20 x 15 cm

Tab.1: Technical data of the frequency doubled Nd:YA10₃ laser for MLRS

A schematic drawing of the proposed technical solution is shown in Fig.1. The laser system consists of a TEM₀₀-oscillator with a double pass amplifier, followed by a frequency doubling system. Nd:YA10₃ crystals are used as the laser medium [1]. Their optical quality as well as their physical properties are comparable to those of Nd:YAG crystals. The main difference is the somewhat longer laser wavelength of the Nd:YA10₃ crystals (1078 nm) and the optical biaxiality, which ensures polarized laser emission and less sensitivity to thermal birefringence.

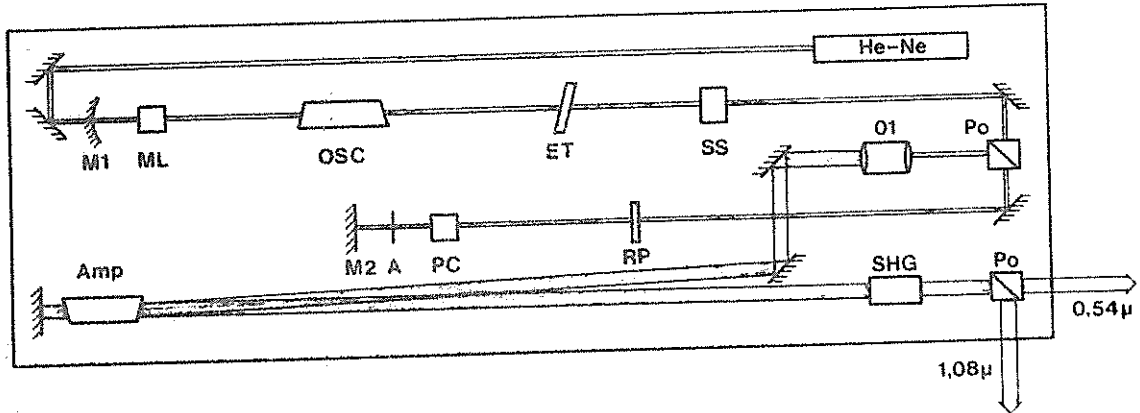


Fig.1 Schematic drawing of the Nd:YA10₃ laser for MLRS.

The resonator of the oscillator is formed by two highly reflecting endmirrors (M1 and M2). Transverse mode selection is achieved by a 2 mm diameter aperture (A). The laser pulse is actively mode-locked by a KD*P electro-optical modulator (ML), its frequency being matched to the total resonator length of 150 cm. The pulse width is controlled by a bandwidth limiting quartz etalon (ET). Q-switching and single pulse selection is done by using the Pockels cell (PC) in the pulse-transmission mode. In order to get a stable mode-locking operation, the system is allowed to pre-lase for several μsec prior to Q-switching by a proper adjustment of the Q-switch voltage.

After switching out the mode-locked pulse from the resonator a telescope (O1) expands the beam 2.5-times to fill the amplifier cross-section. The amplifier (Amp) is used in a double pass in order to reach the required energy level of 30 mJ/pulse. The amplified pulse is then frequency doubled in a temperature stabilized KD*P crystal, and the two wavelengths are separated by the following polarizer (Po).

The electro-mechanical safety shutter (SS) prevents the system from accidental lasing. The same shutter serves also for switching the laser on and off, since the flashlamps are fired at a constant repetition rate of 10 Hz in order to establish well defined thermal conditions.

The active mode-locking concept has two major advantages: First, the buildup of the laser pulse can be easily controlled, synchronizing the Pockels cell with the frequency generator of the mode-locker. The time jitter for pulse emission is reduced down to less than 1 μ sec, resulting in less data to be stored. Second, there are no volatile fluids involved as in case of passive mode-lockers, which could cause serious trouble outside the laboratory.

The MLRS will be operated under adverse environmental conditions. For this reason considerable attention is given to the mechanical and thermal stability of the laser system. The optical bench is a reinforced invar plate, integrated into the cooling system. It is covered by a heavy thermal isolation. All major alignments can be done without disturbing the thermal conditions with the aid of motor-driven differential micrometers integrated to the most important mirror mounts. Built-in photodiodes monitor the performance of the oscillator, the amplifier, and the harmonic generator.

First tests of the laser system will be under way beginning 1982, final tests will be held in the middle of 1982. The MLRS is scheduled to operate for the first time in 1983.

RUBY LASER SYSTEM

This ruby laser system was developed especially for satellite ranging and illumination applications. A first report on the system was given recently by W. Bäuml and K. Nottarp /2/. The specifications are shown in Tab.2. The special feature of the system is the twofold mode of operation:

- i) as a high energy system, emitting 70 J within 300 μ sec for illumination, and
- ii) as a high power system, emitting more than 1 J within 700 psec for ranging.

Mode of operation	Illumination	Ranging
Output energy	70 J	1.4 J
Pulse width	300 μ sec	700 psec
Output power	200 kW	2 GW
Divergence	2 mrad	2 mrad
Repetition rate	1 Hz	1 Hz

Tab.2: Technical data of the ruby laser system at Wettzell, Germany .

The system can be switched from one mode to the other by simple push-button operation. Both modes can be operated at a repetition rate of 1 Hz over an interval of 30 sec. In spite of the relatively large repetition rate, the rubies are kept constant in temperature within 1°C, and, hence, the output wavelength remains within the atmospheric window around 694.3 nm.

A schematic drawing of the laser system is shown in Fig.2. The resonator is formed by a concave highly reflecting endmirror (M1) and a sapphire resonant reflector (M2) for outcoupling. For Q-switch operation a Pockels cell (PC1) and a multiple glass-plate polarizer (Po) is included in the resonator.

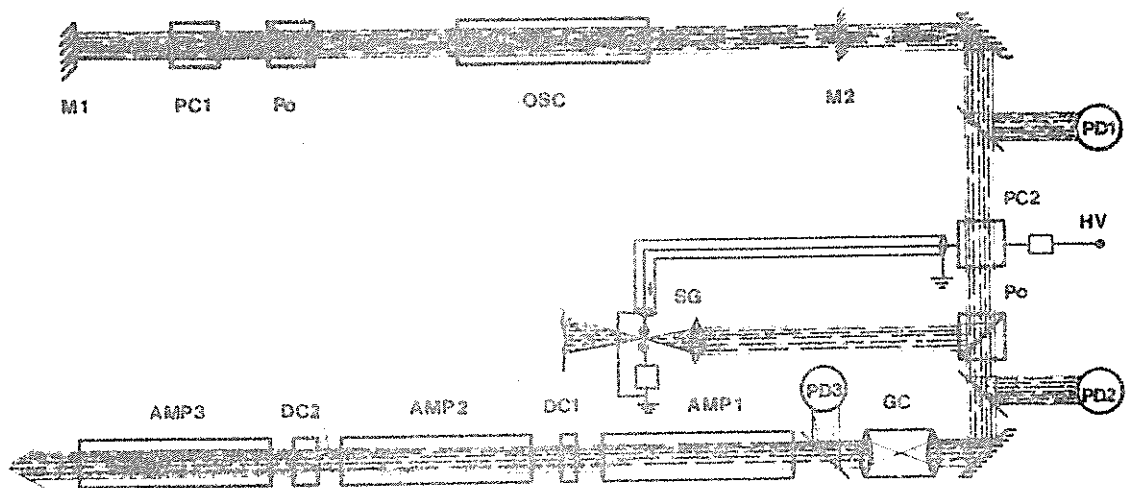


Fig.2: Schematic drawing of the ruby laser system at Wettzell.

Before entering the amplifier chain the oscillator pulse passes the pulse-forming system, which consists of a Pockels cell (PC2), a polarizer (Po), a laser triggered spark gap (SG), and a gas breakdown cell (GC). This system is activated when the laser is operated in the Q-switched mode for satellite ranging. The applied $\lambda/2$ voltage rotates the plane of polarization by 90° and the beam is deflected by the polarizer towards the laser triggered spark gap. By a proper selection of the trigger level one may switch the voltage of the Pockels cell down to 0 V right at the pulse maximum. The transmitted laser pulse has, hence, a very steep rising front. This pulse now enters the gas cell and induces a gas breakdown there. The buildup of the absorbing plasma is extremely fast /3/, transmitting only the very first beginning of the input pulse. The transmitted pulse has a typical pulse width of less than 1 nsec. This pulse is amplified by the following 3 amplifiers, which are optically decoupled by saturable dye cells /4/.

In case of normal mode operation, both Pockels cells are not activated. The laser pulse can pass all the polarizers without deflection. In this case the gas cell has no influence, since the input intensity is well below threshold for gas breakdown. The dye cells are moved out of the light path automatically in order to achieve maximum gain in the amplifier chain.

The performance of the pulse-shaping system is demonstrated in Fig.3. There the Q-switched laser pulse emitted by the oscillator (upper trace), the pulse transmitted by the polarizer (middle trace), and the pulse after passing the gas breakdown cell (lower trace) are shown. These signals were generated by the photodiodes PD1 - PD3, respectively. It is clearly seen how the pulse-shaper acts first on the leading edge and then on the trailing edge of the incoming pulse.

In Fig.4 the pulse shape of the amplified laser pulse is shown on an expanded 1 nsec/div time scale for a single event (upper trace) and for 10 pulses superimposed (lower trace). The reproducibility of the pulse shape is quite remarkable. The amplitude stability is $\pm 10\%$ in 90 % of the shots.

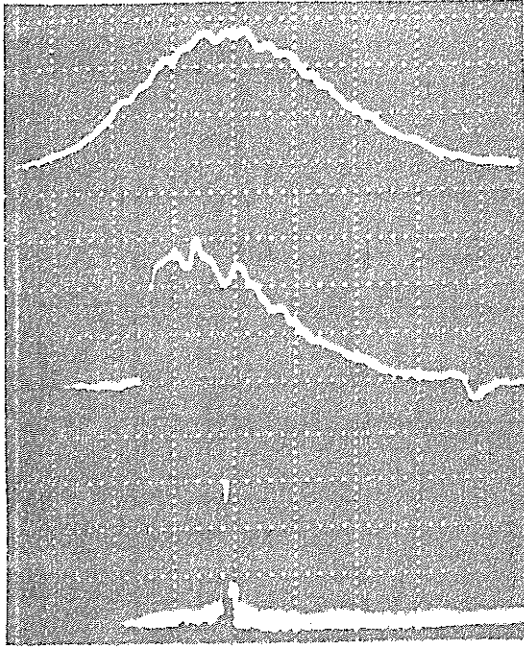


Fig.3 Laser pulse shapes recorded by the photodiodes PD1 (upper trace), PD2 (middle trace) and PD3 (lower trace), when activating the pulse-forming system. Time scale is 10 nsec/div.

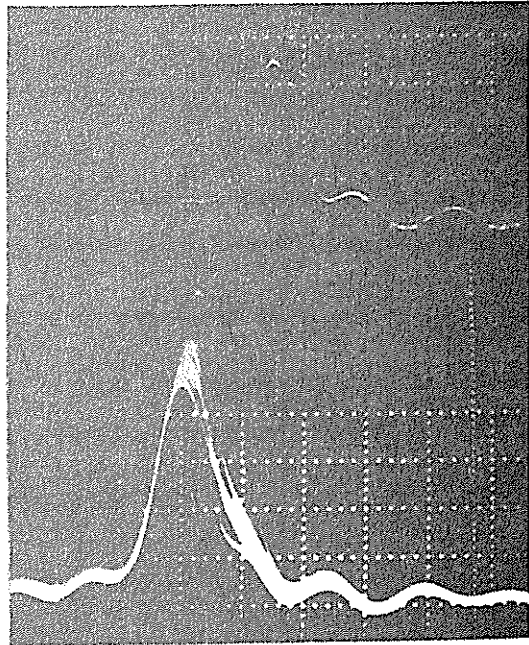


Fig.4 Laser pulses for ranging after leaving pulse-forming system and amplifier chain. Single event (upper trace) and 1 Hz operation superimposed (lower trace). Time scale is 1 nsec/div.

Finally, the subnanosecond pulse duration of the output pulse is demonstrated in Fig.5, where a recording taken by a Tektronix fast transient digitizer is shown. Taking into account the risetime of the photodetector (0.3 nsec) and the bandwidth of the oscilloscope's pre-amplifier (1000 MHz) a pulse duration (FWHM) of 700 psec results.

The above results show that the pulse duration of a conventional Q-switched ruby laser can be reduced from 25 nsec down to 700 psec with rather simple changes. However, it has to be pointed out that powerful amplifiers are necessary to regain the energy lost within the pulse-forming system (at the moment, the energy transmitted by the gas

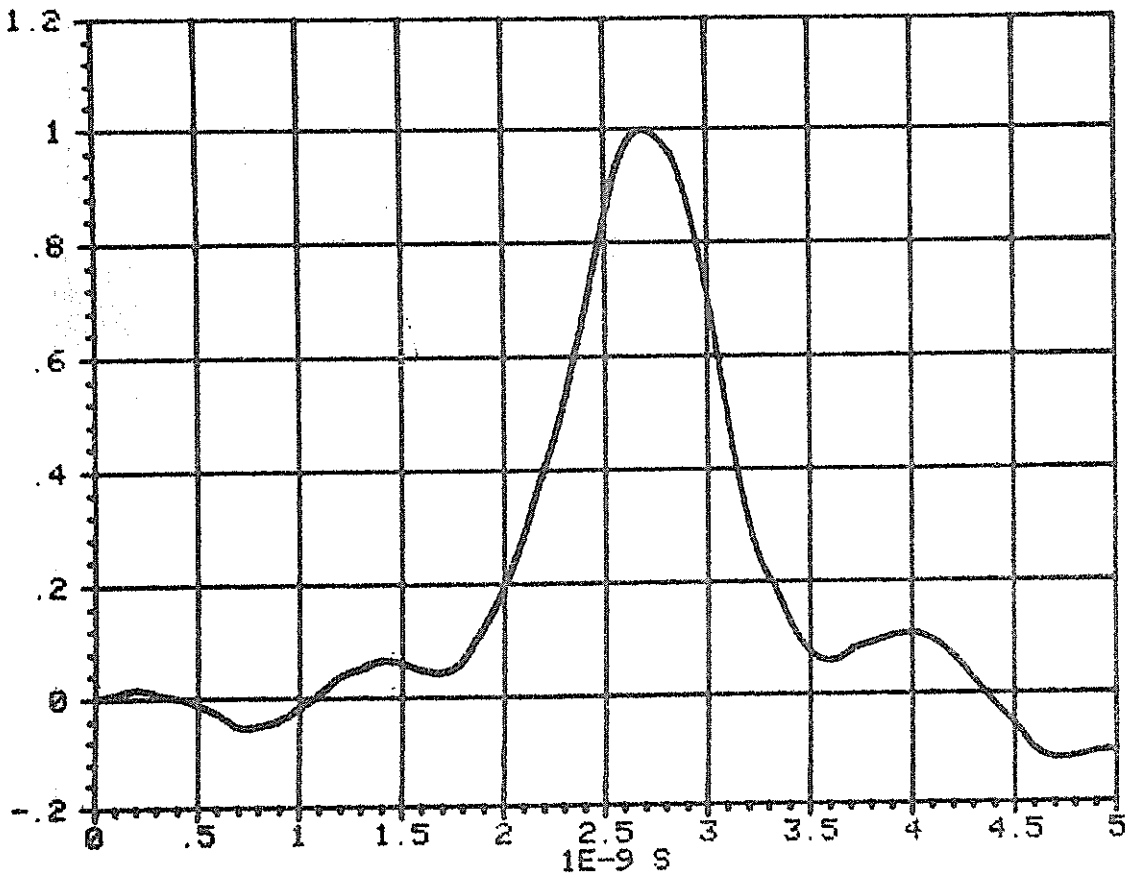


Fig.5 Pulse shape of the ruby laser in the ranging mode.

breakdown cell is of the order of 30 mJ). On the other hand our method certainly has the capability to achieve even shorter pulse durations in the range of 500 psec or less by optimizing the system parameters.

REFERENCES

- /1/ Nd:YA10₃ crystals are manufactured by Kristalloptik Laserbau GmbH
- /2/ W. Bäuml and K. Nottarp, Die Arbeiten des SFB 78 Satellitengeodäsie der TU München im Jahre 1978, pp 40 - 43, Munich 1979
- /3/ H. J. Neusser and H. Puell, Phys. Fluids 15, 1355 (1972)
- /4/ H. Schüller and H. Puell, Opt. Commun. 3, 352 (1971)

LLR TARGET ACQUISITION

B.A. GREENE

Division of National Mapping

NATMAP

PO Box 31, BELCONNEN, ACT 2616
Australia

ABSTRACT

The problem of target acquisition in Lunar Laser Ranging (LLR) is discussed. The effectiveness of each guiding mode will be influenced by the response time and sensitivity of the real time analysis (RTA) used to indicate success. Without an absolute pointing capability of 3 arc seconds, the optimum guiding mode may vary with respect to moon phase, and for each mode suitable RTA must be provided.

The role of RTA in system ergonomics is emphasised, and an extremely sensitive method which is suited to all guiding modes and meets the requirements of human operators is confirmed.

1. Introduction

The application of single photoelectron detection (SPE) in satellite laser ranging (SLR) systems has recently reduced the number of problems unique to lunar laser ranging (LLR) systems. Those SLR systems operating with SPE generally employ full aperture transmission, narrow beam divergence, and precision tracking to reduce the laser power required for the ranging operation to a level which is not liable to cause eye damage. Thus there has been a convergence of LLR and SLR technologies in:

- (a) detectors
- (b) guiding and pointing
- (c) data analysis
- (d) system calibrations
- (e) receiver filtering
- (f) control systems technology

Concurrently, there has been a reduction in emphasis on aircraft detection and high power lasers in current SLR design - both of which continue to be of interest for LLR systems.

This paper will deal with the problem of target acquisition in LLR - a problem which remains identifiably different from SLR and which requires consideration of many aspects of system design ranging from laser and computer selection to system ergonomics.

2. Guiding Modes

There are several ways of tracking a target at the 3 arc second level for laser ranging. The most common methods are:

(a) Absolute Pointing and Tracking

If the target position at any time is known to better than 3 seconds of arc, and if the LLR telescope can point with equal precision, then the target can be acquired directly. The advantage of this method is that it is independent of target visibility (ie moon phase) and can be used for daylight ranging when even visible targets lose contrast and are difficult to track optically. No LLR currently operates in this mode.

(b) Relative Pointing

Systems which have no ability to point within 3 arc seconds absolute error may have a capability for very precise relative pointing over short angular distances. Thus if a well defined target (star or crater) which is angularly close to the laser target can be acquired, the telescope can be made to drive precisely to the target position.

(c) Imaging Devices

A telescope with only coarse pointing capabilities may make use of electronic imaging devices which 'recognize' the target area and provide drive input to maintain the telescope on target.

(d) Manual Acquisition

By viewing the target area from an optical system (eyepiece, TV) accurately boresighted with the telescope, an operator can control the tracking rates to keep the telescope on target if he is familiar with target area moonscapes.

The systems (a) - (e) may be associated with 'search' programs which scan the area around the commanded position in search of target returns. For all systems, criteria for successful ranging must be defined in terms of tests on the received data, so that the tracking

system can cease searching and lock onto the target.

3. Real Time Analysis

The laser ranging system should incorporate a real time analysis (RTA) facility to provide an indication that the ranging system is on target. The response time required for this analysis will be related to the occupation time of a point on the search grid and the response time of other units in the feedback path. Indeed each guiding mode should be designed as a closed loop servo system with full consideration of the bandwidths of each component.

The flagging of ranging success by a RTA unit has uses beyond locking onto the target. A continuous indication of ranging performance is satisfying and reassuring to the system operators, and minimises unnecessary and often derogatory manual adjustments to 'enhance' performance.

The RTA method used is constrained by almost every aspect of system design, and the requirement for RTA will have an influence in operating parameter selection. Clearly, the difficulty in detecting signal in real time will be related to the SNR in logged data. Using a dot display of residual vs time and a human operator as discriminator (1) is extremely sensitive and efficient. Extensive simulation (2) indicates that signal can readily be detected with this system for SNRs as low as 0.05.

Fully automated algorithms for defining 'on' and 'off' target are less sensitive than this when constrained to run in real time with large (100's of ns) uncertainties in range prediction. If background resident, which is most effective from a system operations viewpoint, the 'RTA' may increasingly lag the data acquisition. When an LLR is fully operational the uncertainty in the range should be much less than 100 ns, in which case an entirely machine resident RTA might be expected to manage easily. However, this is not so, since unobserved timing system (epoch) errors, systematic error changes, atmospheric error fluctuations, and other variable biases make it undesirable to make rigid a priori range estimates. In fact it is occasionally the range residual (predicted minus observed range) which can indicate timing and other system errors.

Thus it is most desirable to have the most sensitive possible RTA, such that signal can be detected in very moisy environments as quickly as possible. Clearly the response time for RTA need not be less than other system time constants, however it is also clear that excessively slow or insensitive RTA will prolong search pattern execution.

4. SNR Selection

The SNR in data can be selected by the system designer. The parameters controlling this factor are shown in Figure 1.

The worst case design will be for full moon (maximum noise) ranging. The moon phase dependency of receiver noise can be approximated by a squared sinusoid, with noise proportional to $\sin^2 (D/28)$, where D is the number of days since the start of the lunation.

The SNR can be made high by selecting (eg) a high laser pulse energy. However, maximum productivity for the system is associated (through another optimisation process) with maximum mean laser power, and the highest mean powers currently available are for 10 Hz (typically) pulse repetition frequencies. Thus, if tradeoff is to be avoided between guiding efficiency and productivity, the RTA should be made sensitive enough to detect signal at full moon using a maximum mean power laser.

Since the most sensitive RTA currently available will not give high confidence level success indication for SNR below 0.05 within 100 data points, the system designer is obliged to tailor the SNR to suit, or to sacrifice some observations. This is done by using established range equations and varying control parameters as indicated in Figure 1.

5. Effect of Atmosphere

For LLR, the transmit and receive optical axes should be within (about) 3 arc seconds of the target. The atmosphere plays an important role in the pointing process by adding random walk to both the transmit and receive optical axes. The large travel time (3 seconds) results in decorrelation of the transmit and receive axes by as much as the value of atmospheric seeing, which has 100 ms time constants. This can be modelled as a degradation of SNR by a factor of $(S/2)^2$, where S is the seeing in seconds of arc.

Similarly, for ruby lasers, the effect of precipitable water vapour can be approximated by an SNR degradation factor of $(W/3)^3$, where W is the precipitable water vapour in mm.

Thus if a system is to function satisfactorily in 6 arc seconds seeing with 6 mm of water in the atmosphere, the SNR for perfect conditions must be 32 times the threshold value.

The formulae for obtaining the factors are simple approximations, and based on observations of LLR data. The observations that no data at all has been observed in LLR for S greater than 8 or W greater than 9 is not incorporated into the models. More sophisticated models based on large data volumes will soon be possible as high productivity Nd:YAG systems become established.

6. Conclusion

The LLR system designer must clearly define the operating envelope for the system in terms of moon phase, atmospheric, and other considerations. He must then ensure that in operation, the SNR is within the limits imposed by available RTA, since if the guiding is not within specification, a potentially high productivity system will yield no results.

A high degree of awareness in the system operators of the influence of various parameters especially meteorological, on SNR is desirable to avoid false expectations which can corrupt the target acquisition process.

References

1. J. Rayner, Proc. Third International Laser Ranging Workshop, Lagonissi, Greece, May 1978.
2. R. Bryant, National Mapping unpublished report.
3. E.C. Silverberg, 'The Parameterisation of the Accuracy of a Lunar Laser Ranging System' University of Texas Res. Mem. 77-001, January 1977.

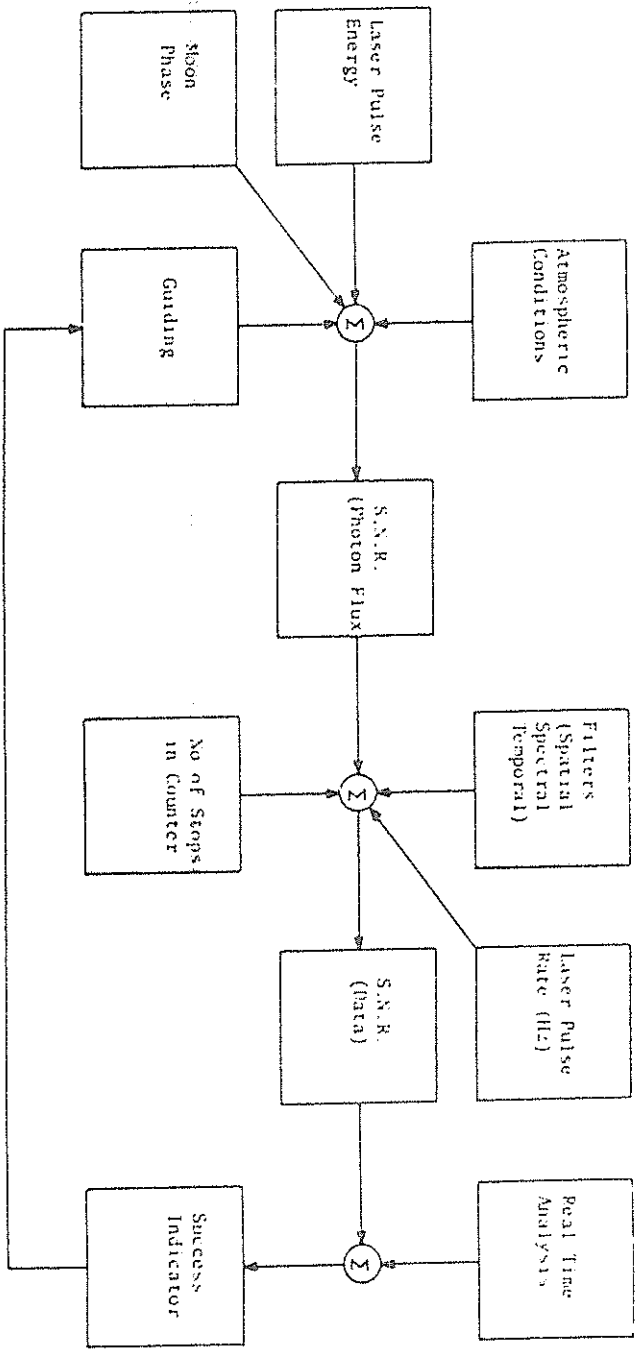


Fig 1. GUIDING CONTROL LOOP

DESCRIPTION AND FIRST RESULTS
OF THE CERGA LUNAR-LASER STATION

by J.F. MANGIN, Ch. DUMOULIN, J.M. TORRE,
J.L. SAGNIER, J. KOVALEVSKY, D. FERAUDY
CERGA, Grasse, France

I - INTRODUCTION

A preliminary description of the CERGA lunar laser was given in the Lagonissi Laser Workshop (O. Calame and J. Gaignebet, Laser Workshop, Athenes, p. 139, 1960). The main features described three years ago have not changed. The aim of this presentation is to give some supplementary information on some sub-systems and to present the observing procedure that is adopted and had permitted to obtain the first returns.

The telescope (see M. Bourdet and Ch. Dumoulin in the present proceedings) is used for the three basic functions : emission, reception and tracking. The three corresponding optical paths are schematically described in figure 1.

II - EMISSION

Presently, the laser gives an impulse with a 3 ns width at half intensity. The mean energy is 2.5 Joules. The emission optical system includes three treated lenses, six mirrors and a dichroic mirror, three of which are treated for high energy impacts. The total loss in energy is estimated at 30 %, so that the outgoing energy is 1.75 Joule.

The natural divergence of the laser is $\pm 1''5$. The accuracy of the focalization of the telescope - coupling lens system is also estimated $\pm 1''5$. Presently, the observed defect of the secondary mirror (the glass was attacked during a treatment) is of the order of 4".

If we take 3" for the turbulence effects, we estimate to 5"5 the diameter of the beam on the Moon. A reduction to a little more than the spreading due to the turbulence is expected when the secondary mirror will be replaced.

III - RECEPTION

The return photons are reflected by the three mirrors of the telescope, the dichroic mirror, two other treated mirrors and then go through two lenses before reaching the photocathode. The gross effect of the transmission of the optics and of the quantic efficiency of the photomultiplier gives an overall transmission factor of 4.5 %. This was checked on stars, using a large (12") diaphragm. Smaller diaphragms (8", 5", 3", 2") are also available. Four successive events may be timed by the event-timer during the opening of the electronic gate.

IV - TRACKING

A beam splitter situated behind the dichroic mirror directs a part of the incoming beam for direct guiding using a reference reticle. Another part is sent in a TV camera. An offset device can drive the camera in a precomputed manner, so as to permit an offset guiding on a given crater, while the telescope is still pointing the retroreflectors.

At present, the offset guiding is not in service and the following procedure is used :

1. A given crater is tracked using reference ephemerides
2. The camera is centered on the crater and the offset in azimuth and elevation Δa , Δe are noted
3. The telescope is pointed blindly on the reflector using the ephemerides and the corrections Δa and Δe are applied. These corrections are essentially due to telescope flexures and other mechanical irregularities. Some of them have been empirically represented by trigonometric expressions, and the corresponding errors as well as a refraction model are included in the software control of the telescope.

The time necessary to execute these three steps is approximately 7 minutes. They are followed by a series of about 70-100 firings lasting another 7 to 10 minutes.

V - FIRST RETURNS OBTAINED BY THE STATION

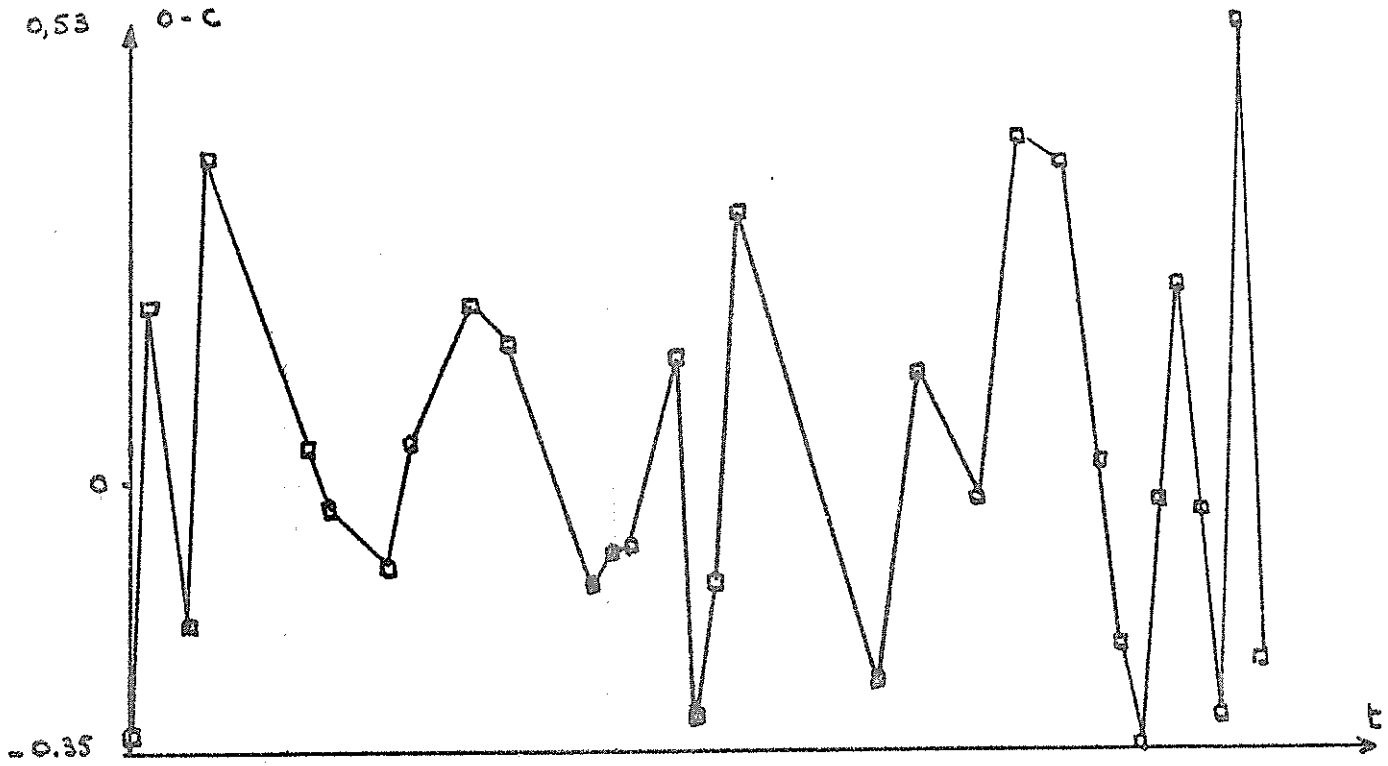
A few series of returns were obtained during the summer of 1980 on GEOS 3 and STARLETTE. For instance, on the first of July, 49 events were obtained after 40 laser firings. Out of them 31 were retained as being returns with an internal consistency of ± 25 cm (fig. 2).

The first returns on the Moon were obtained on June 8th, 1981, when two series of 7 events were recognized as probable returns. The number of noise events received during the 7 minutes corresponding to the 80 laser shots were respectively 60 and 40 for a gate width of 10 microseconds.

Another result was obtained on July 7th, when from a first glance on 50 events, one could recognize 19 as probable returns (fig. 3). Three of them have residuals with respect to a linear function of time (due to UT1-UTC effect) of the order of 10 ns. This offset is now being studied, but has not yet been understood. The mean quadratic error of the remaining 16 returns is ± 1.5 ns (or ± 22 cm).

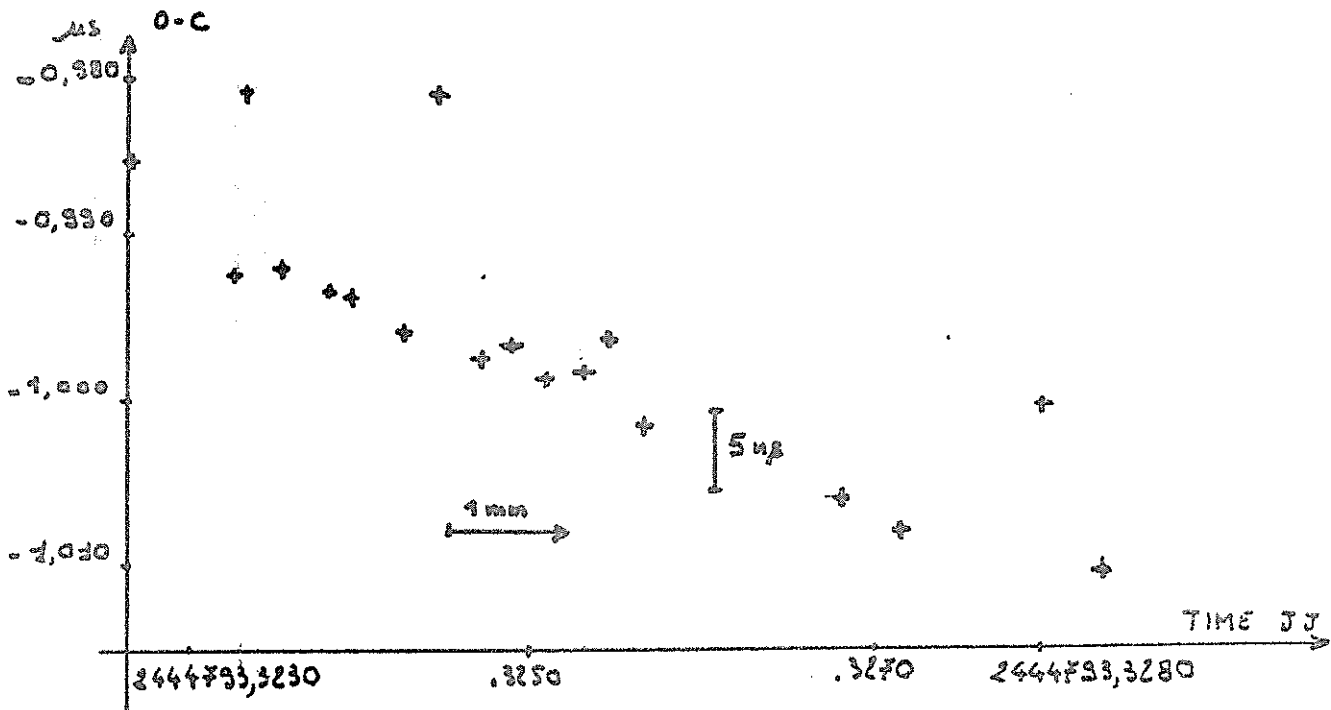
Presently only observations on Apollo 15 reflectors during lunar nights have been attempted. A significant improvement in the efficiency of the station is expected when a new secondary mirror and a narrower filter will be available.

The first returns have been confirmed by some other series in November 1981.



o - c of the 31 events obtained on GEOS 3 by the Cerga Luna Laser
July 1st 1980

Fig. 2



o - c of the 19 events obtained on the Moon by the Cerga Luna Laser
on July 7th 1981

Fig. 3

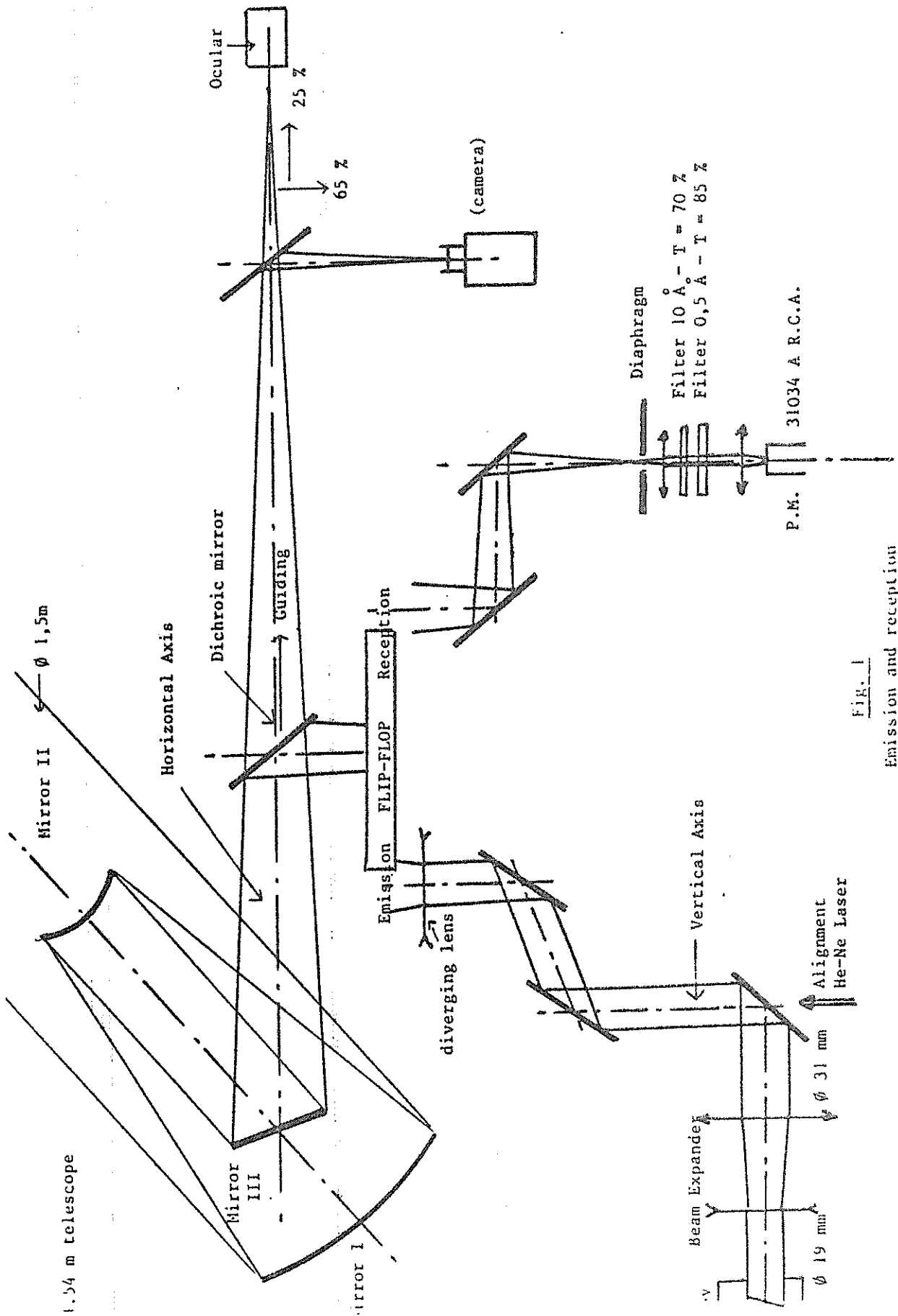


Fig. 1

Emission and reception configurations of the Cerga lunar laser.

McDONALD LASER RANGING OPERATIONS
PAST, PRESENT, AND FUTURE

by

Peter J. Shelus and Eric C. Silverberg
Department of Astronomy and McDonald Observatory
University of Texas at Austin
Austin, Texas 78712 USA

ABSTRACT

The 2.7-meter lunar laser ranging system at McDonald Observatory in West Texas has been in regular operation since mid-1969. It has been the major source of LLR data since that time. We are now in the final stages of construction of a stand-alone, dual-purpose laser ranging station to replace it. Herewith is presented some of our accomplishments of the past and some of our expectations for the future.

1 INTRODUCTION

We are rapidly approaching the end of an era with lunar laser ranging as we begin the process of phasing out LLR operations on the 2.7 meter reflector at McDonald Observatory in west Texas. Over the past twelve years this station has been continuously and routinely operating to obtain the overwhelming percentage of the world's high accuracy lunar range data. This feat becomes even more remarkable when one considers the fact that this has been accomplished even though the experiment has been constructed around, and makes constant use of, a standard telescope which is scheduled 24 hours a day, 365 days per year for normal astronomical activity. The definitive document for the station continues to be that of Silverberg (1974).

The day-to-day operations, as well as most system problems, modifications and upgrades, have been chronicled in the station reports which were issued thrice per year under NASA Grant NGR 44-012-

165. With the demise of that grant and the transfer of McDonald Observatory laser ranging operations to NASA Contract NAS 5-25948, the reports on day-to-day activities continue to be made in the regular monthly submissions as well as in the documentation which accompanies the semi-annual data deposits into the National Space Science Data Center, i.e., Shelus (1981). All of these reports and documents have received wide distribution and should be readily available to all interested parties.

The operational philosophy of the McDonald LLR station has been a unique one. This philosophy is probably, in large part, responsible for the fine level of success which the station has experienced. Because of the fact that the station has always been considered to be an "operational" one (even initially) instead of one established primarily for research and development, it has always been expected that data would be gathered under all but the most pressing of circumstances. Day-to-day problems have always received the primary attention of observatory staff members and all modifications and upgrades have been handled such that regular observing schedules are seldom compromised. Further, changes have been made in ways which do not force the immediate abandonment of older equipment and/or techniques; a change which proves to be problematical can be quickly rescinded and original operational procedures can be resumed while such changes are "debugged". The result of such an operational philosophy has been such that in the many years of 2.7 meter LLR activity at McDonald Observatory, only for a telescope drive spur gear change in September, 1972 has the station been continuously out of operation for more than a week.

Further, the aim of the McDonald LLR station has not been simply that of data gathering. A firm commitment has been made concerning the observational data obtained. If such data is not made available to the general scientific community in a timely manner, together with all clock, calibration, environmental and ancillary data, the scientific relevance of the experiment has been lost. To this end, the station has been molded to provide all relevant data to researchers with a minimum of delay and in a standard, well-defined machine-readable format. Success has been encountered here as well since all data is provided to the user, either through direct mailing, electronic data transmission or regular NSSDC deposits. Monthly distributions of filtered data and normal points are made within approximately six weeks of observation and semi-annual NSSDC deposits are made within approximately three months of observation.

2.7 METER LLR SYSTEM

As has already been mentioned, most of the relevant material dealing with the 2.7 meter LLR operations at McDonald Observatory has been provided by Silverberg (1974). Figure 1 schematically depicts

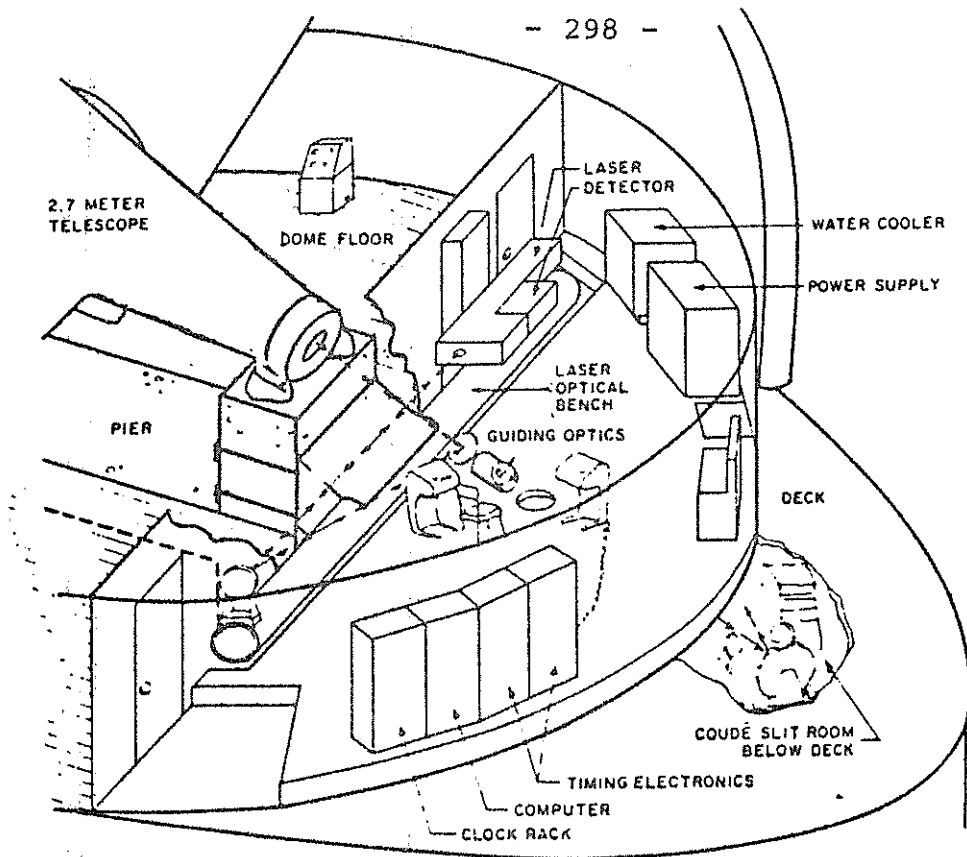


Figure 1.

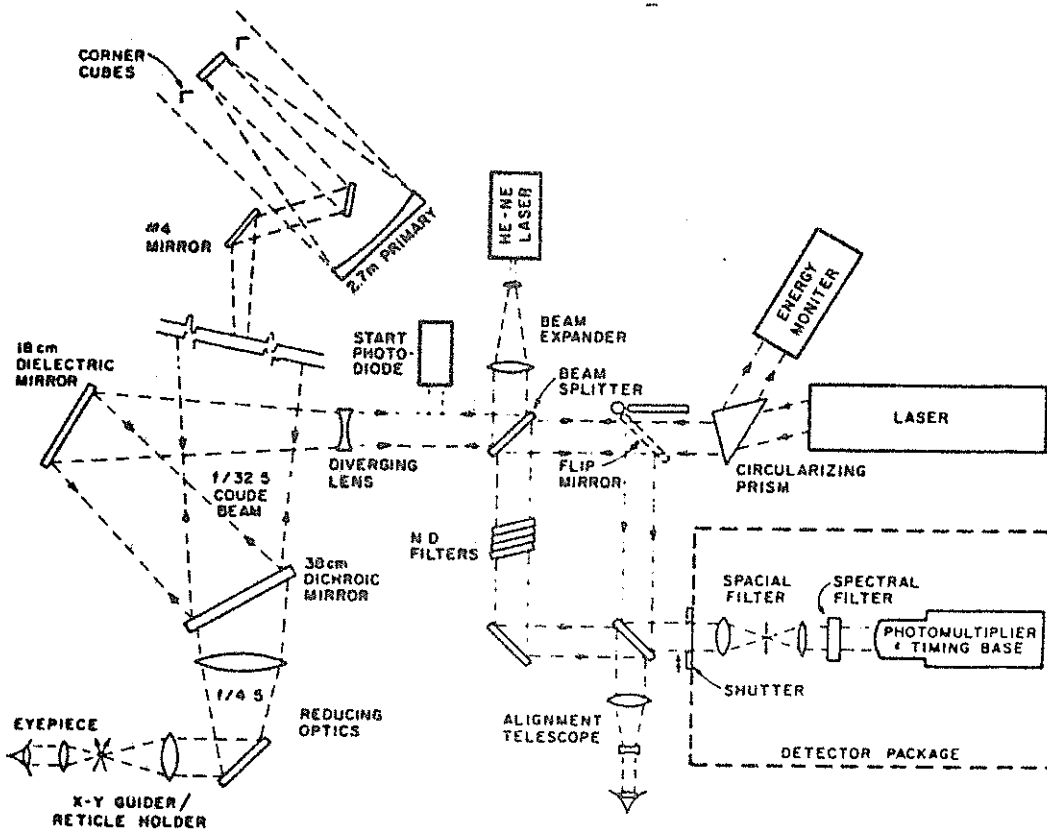


Figure 2.

the present configuration in the telescope dome. Figure 2 shows the major optical components which are used in conjunction with the 2.7 meter telescope. Table 1 gives the relevant McDonald LLR hardware specifications. Laser ranging operations are performed thrice daily on approximately 21 days per lunation. Forty-five minute observing sessions are held when the moon is approximately 3 hours east of, on, and 3 hours west of, the meridian. Each forty-five minute session is spent in obtaining ranges from one or more of the lunar surface retroreflectors (one at a time, of course). Calibration information is obtained in real-time as observations are being made; clock data is archived automatically through the month to allow the recovery of UTC from the station clock; environmental and ancillary data is recorded on the log.

Once a lunation (more often, under special conditions) a magnetic tape of all related LLR information is forwarded to Austin for filtering, reformatting, compression, archiving and distribution. Table 2 summarizes observing statistics by year and by reflector; Figure 3 gives statistics on the data compression ratio; Figure 4 presents statistics of uncertainty estimates for the McDonald data set; Figure 5 summarizes normal point distribution with respect to the classical fundamental arguments of the lunar theory; Figure 6 gives information on the distribution of McDonald LLR data with respect to lunar local hour angle and declination.

3 McDONALD LASER RANGING SYSTEM - MLRS

At the present time we are in the process of establishing a new laser ranging station at McDonald Observatory. Unlike the present 2.7 meter system, the new station will be dedicated to laser ranging operations, and it will have the capability of ranging to lower (artificial) satellites as well as to the moon. Basic operating parameters of the MLRS can be found in Table 3. A line drawing which depicts its major components is found in Figure 7.

Although this station has been developed as a stand-alone replacement to the 2.7 meter LLR system, it has made extensive use of systems and procedures which were developed for the Transportable Laser Ranging Station. The TLRS is a very compact, mobile LAGEOS laser ranging station now in regular operation in the western United States under the NASA Crustal Dynamics Project. Timing electronics, photo-detector and calibration procedures are identical to those of the TLRS. The system software is also very similar to that of the TLRS with the major differences concerning the lunar versus LAGEOS capabilities. The system contains a dual laser and lunar guiding is performed using a dichroic #3 mirror. Many of the hardware and software components of the TLRS/MLRS systems are being presented in various sessions of this Workshop. The interested reader should refer to the appropriate parts of the formal Workshop Proceedings for

TABLE 1

McD 2.7-m LLR Operating Parameters

APERTURE	2.7 m
MOUNT	EQUATORIAL
AV. POWER	0.4 w
DIVERGENCE	1.5 arcsec
WAVELENGTH	694.3 nm
PULSEWIDTH	3 nsec
REP RATE	1/3 Hz
SPATIAL FILTER	6 arcsec
SPECTRAL FILTER	0.7 Å

TABLE 2

Number of McD Normal Points

YEARS	0	2	3	4
1969	2	0	0	0
1970	57	0	0	0
1971	84	74	73	0
1972	54	58	247	0
1973	72	85	277	1
1974	40	53	212	24
1975	36	46	250	32
1976	39	34	229	17
1977	15	14	203	14
1978	14	21	166	21
1979	11	23	111	8
1980	31	58	201	4
Jan-Jun 1981	14	18	82	5

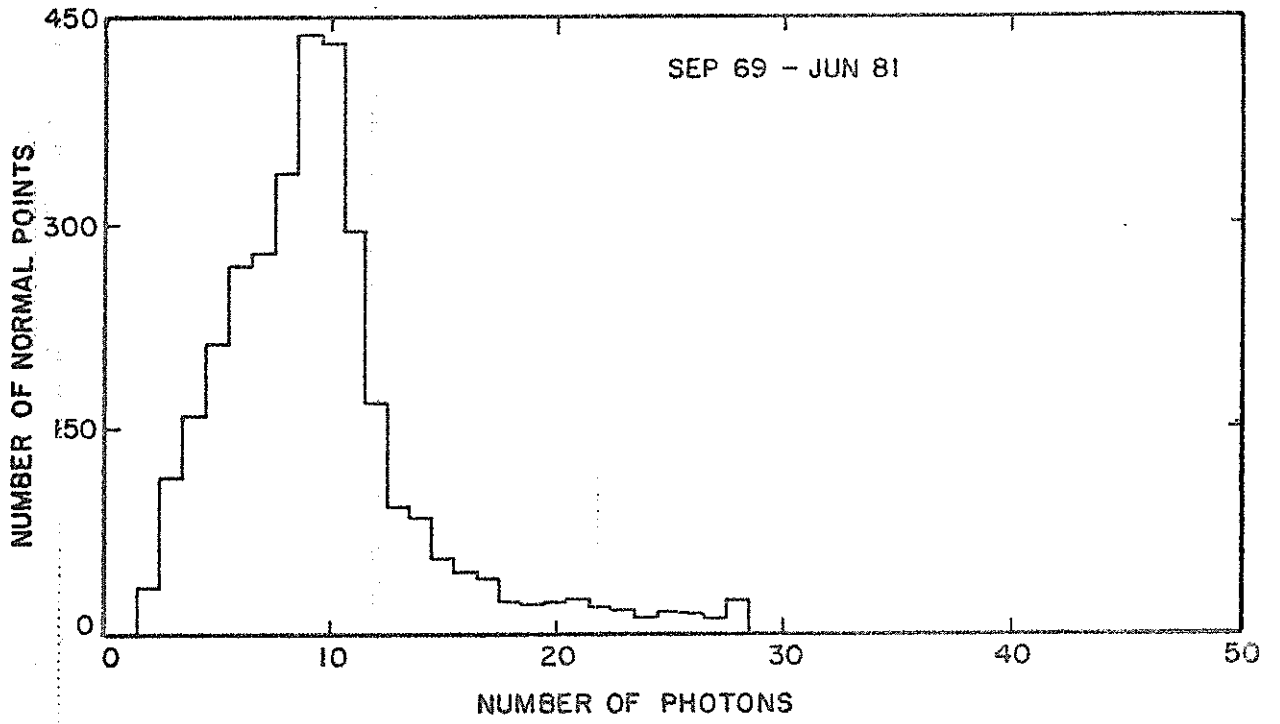


Figure 3.

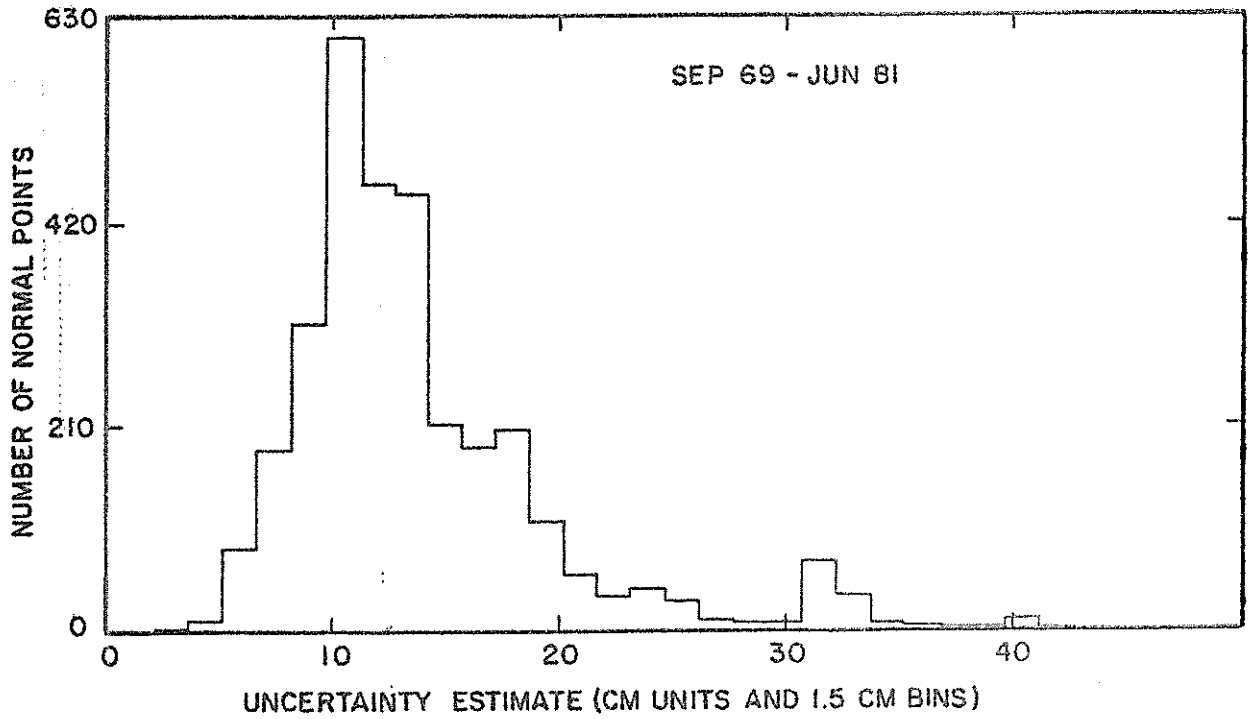


Figure 4.

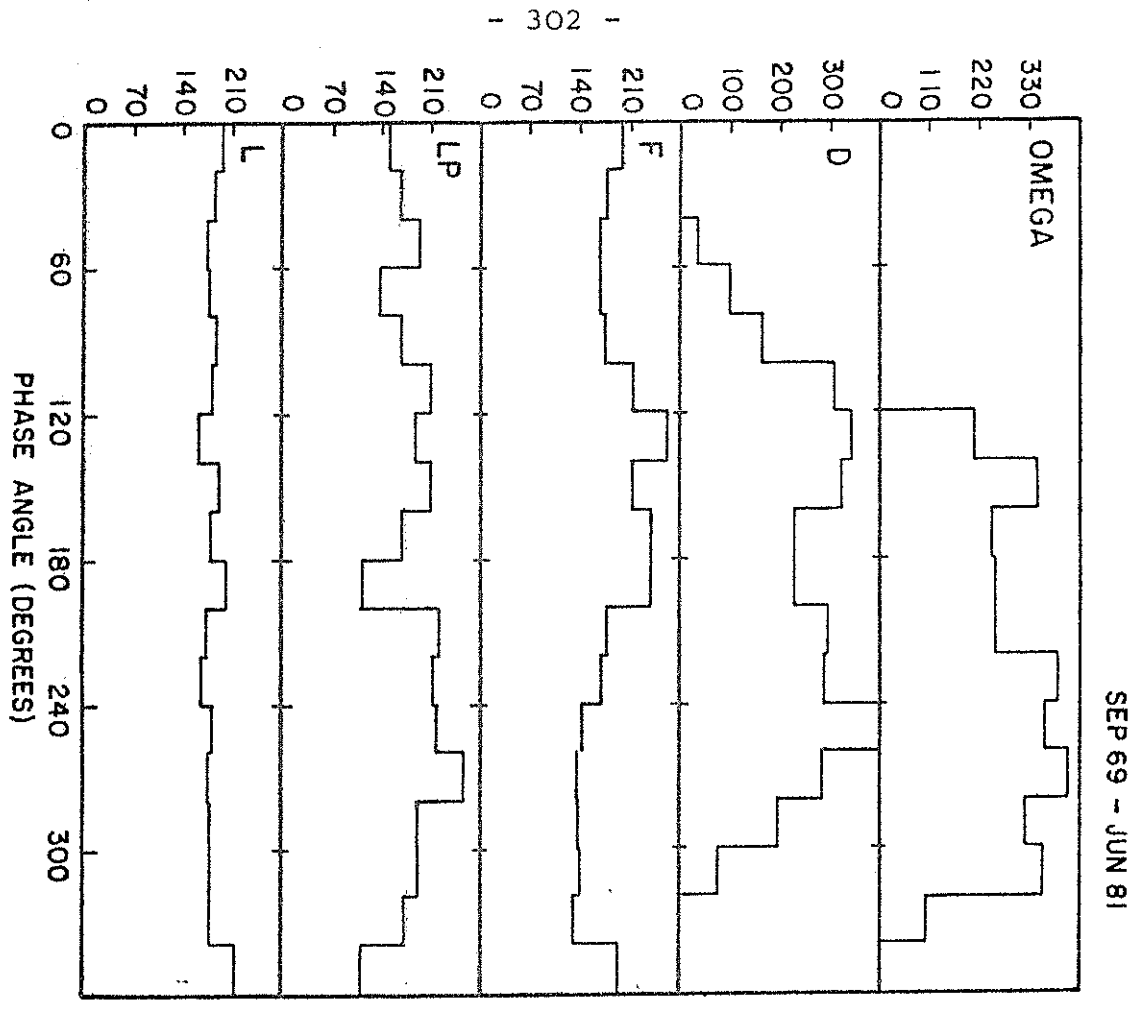


Figure 5.

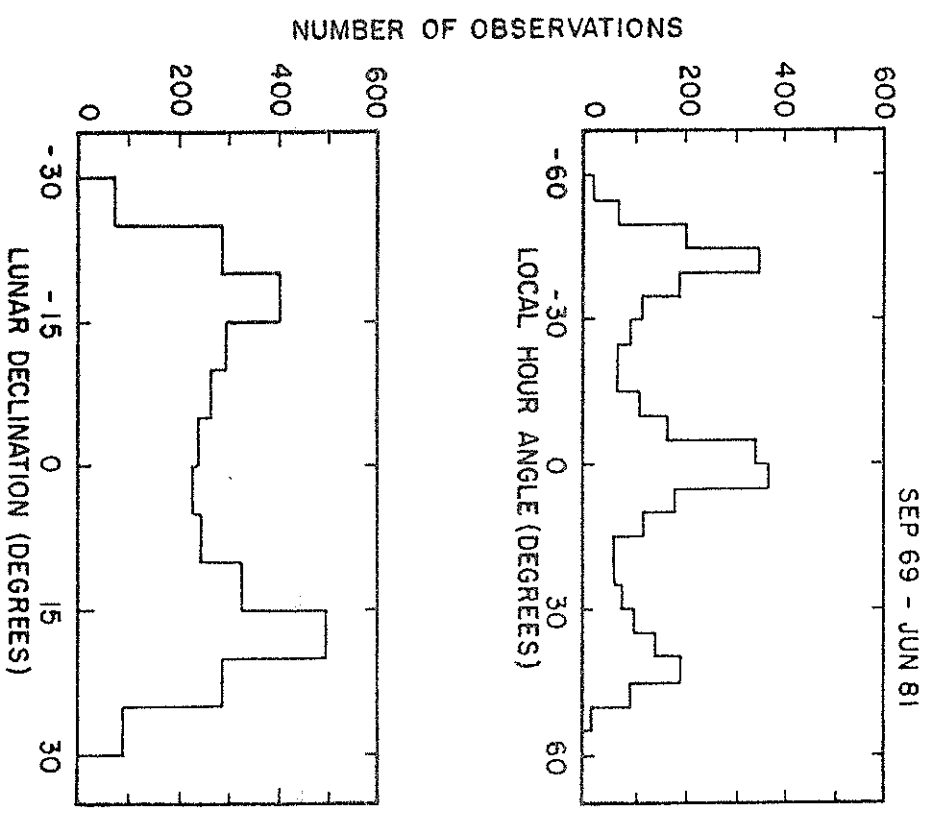


Figure 6.

TABLE 3
MLRS OPERATING PARAMETERS

	<u>LAGEOS</u>	<u>MOON</u>
APERTURE		0.76 m
MOUNT		ALT-ALT
AV. POWER	-10 mw	4-5 v
DIVERGENCE	-10 arcsec	~3 arcsec
WAVELENGTH		532 nm
PULSEWIDTH	0.1 nsec	3 nsec
REP RATE		10 Hz
SPACIAL FILTER	6-40 arcsec	6-12 arcsec
SPECTRAL FILTERS		0.8, 3, 10 Å

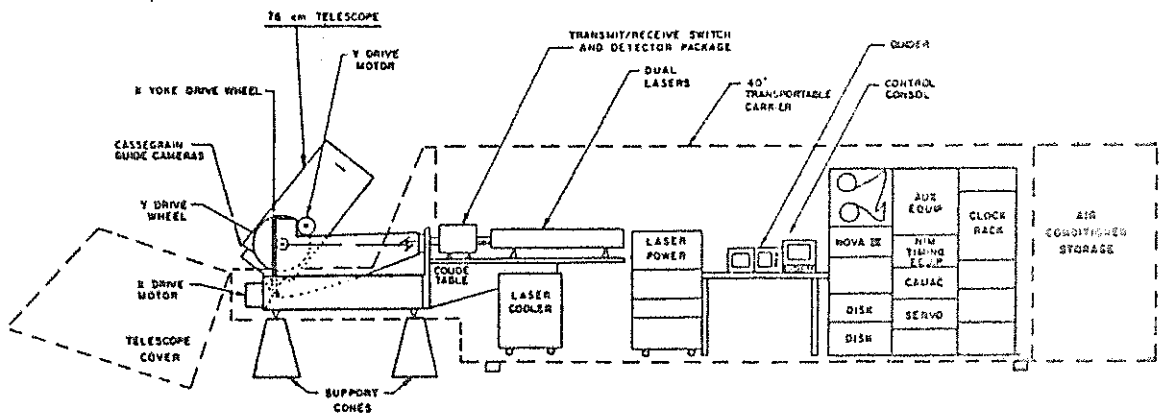


Figure 7.

further information concerning them.

As the system is presently envisioned the system is software intensive having been built around a sophisticated Data General Nova-based operating system. This operating system should be able to furnish computer support throughout all routine observing sessions from computing point angle and ranging predictions, pointing the telescope and firing the lasers, performing necessary calibration and clock maintenance; recording environmental data; and, finally, filtering, compressing and reformatting the data for data distribution.

4 CONCLUSIONS

A long and successful history surrounds LLR activity at McDonald Observatory. Many of the lessons which have been learned from the original 2.7 meter system and the TLRS mobile station are in the process of being incorporated into the new MLRS system. We feel that our basic philosophy of an "operational" station is important to successful operations). Many of the hardware aspects of the old and new stations have appeared in the Proceedings of earlier Laser Workshops as well as in those of the current Workshop. Many of our software algorithms are being presented during the Software sessions of the present Workshop here in Austin. We are looking forward to successful operations of the MLRS in the very near future.

5 ACKNOWLEDGEMENTS

The current McDonald Observatory lunar laser ranging operations are funded under NASA Contract NAS5-25948. The basic funding for the construction of MLRS comes from NASA Contract NASW-3296.

6 REFERENCES

- Silverberg, E. C. 1974, "Operation and Performance of a Lunar Laser Ranging Station" Applied Optics, 13, 565.
- Shelus, P. J. 1981, "Lunar Laser Ranging Data Deposited in the National Space Science Data Center - Normal Points, Filtered Observations, and Unfiltered Photon Detections for 1 January 1981 through 30 June 1981", UT Res. Memo. in Astronomy, October, 1981.

GENERAL HARDWARE/SOFTWARE ORGANIZATION

by J.M. TORRE and J. KOVALEVSKY
CERGA, Grasse, France

I - GENERAL DESCRIPTION

The CERGA lunar-laser ranging system as described by J.F. Mangin et al. in these proceedings has been set up in such a way that the telescope control is strictly separated from the real time control of the ranging experiment. Consequently, two different computers are used in a completely independant modes. These are :

1) Data general "Eclipse 5200"

- CPU with 64 K byte
- Disk unit
- Alphanumeric Tektronix display
- Texas Instrument SILENT 700
- TTY
- 16 bits interfaces (digital I/O)
- RS 232 C interfaces (asynchroneous line multiplexes)

Software support : Real time disk operation system
FORTRAN 4

2) Data General "Nova 1220"

- CPU with 16K byte
- TTY
- 16 bits interfaces (digital I/O)
- RS 232 C interfaces (universal line multiplexes)

No software system. Machine language coding.

The various hardware subsystems that are linked with these two computers are schematically described in figure 1.

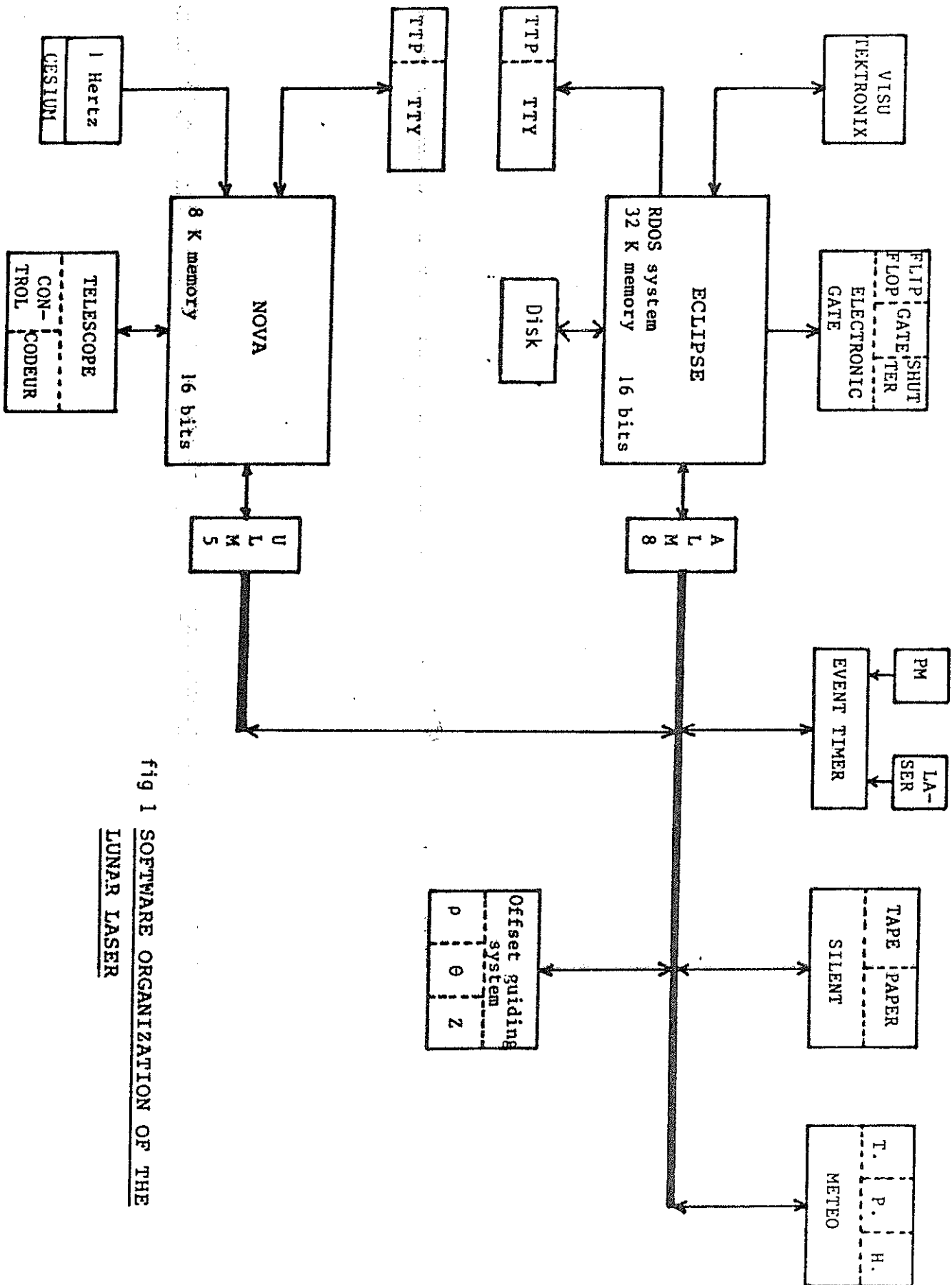


Fig 1 SOFTWARE ORGANIZATION OF THE LUNAR LASER

II - COMPUTER ORGANIZATION

Four different functions are executed by these computers. Let us describe them.

1) Ephemeris treatment

The ephemerides of reflectors and reference craters are computed by O. Calame on the CNES CDC computers and transferred on cassette compatible with Texas Instrument Silent. These cassettes are read by the Eclipse computer and filed in the disk. Each cassette contains the ephemerides for about two weeks of observation.

Presently, before each observation, the ephemerides of the selected reference craters and of the reflectors are transcribed by the Eclipse on a paper tape, in a form that can be read by the Nova. In the future, it is contemplated to transfer these ephemerides directly from Eclipse to Nova through both RS 232 C connections.

2) Pointing and tracking

When the decision is taken by the observer to track a crater (or a reflector), the corresponding paper tape ephemerides are read by the Nova computer. It interpolates the apparent positions for every second. A 1 Hertz top provided by a cesium clock synchronizes the orders prepared by the computer and sent to the telescope. The link is made through a 16 bit input/output interface.

In the future, we intend to use an offset guiding so as to control the tracking by a crater observed with a TV camera, while the telescope is pointed at a reflector. It will be controlled by the Eclipse computer, linked to the offset guiding system by the RS 232 C interface (asynchronous line multiplexor ALM 8).

3) Real time control

The Eclipse computer linked to the event-timer through the ALM 8 records the time of the firing. Then, it computes and transmits to the electronic gate the expected time-delay between the instant of the firing and the return event.

Then, the Eclipse, reads on the event-timer the times of the events and compares them with the ephemerides. The residuals are computed and a histogram of the number of residuals in given time channels is displayed on the Tektronix screen.

4) Quick-look data evaluation

After the series of laser shots are over, it is possible to analyse all the delays obtained and construct histograms with various channel widths. The number of events for each 5 ns channel is printed on the teletype. The probable returns as shown on histograms are then treated by the Eclipse, and recorded on cassettes with other parameters (meteorology, noise, etc...) for scientific treatment. A mean quadratic error of the selected probable returns is computed and the corresponding observations and residuals are printed. This allows the observer to be aware of the quality of the observations a maximum of 5 minutes after the last laser shot.

LUNAR AND PLANETARY EPHEMERIDES: ACCURACY,
INERTIAL FRAMES, AND ZERO POINTS

J. G. WILLIAMS

JET PROPULSION LABORATORY
CALIFORNIA INSTITUTE OF TECHNOLOGY
PASADENA, CALIFORNIA 91109

A new lunar and planetary ephemeris has recently been completed. I would like to briefly describe the accuracy of this ephemeris and to argue that such modern ephemerides are closely related to an inertial coordinate system. The ephemeris has a definable and repeatable zero point. It would be desirable to tie the VLBI frame together with the lunar and planetary celestial frame and to connect the terrestrial frames of the lunar and LAGEOS laser ranging systems.

The new JPL planetary/lunar ephemeris comes in two versions designated DE200/LE200 and DE119/LE63. The coordinates are on the equator and equinox of J2000 and B1950.0 respectively. Both are on a dynamical equinox and they differ from one another only by a rotation. The ephemerides result from joint integrations based on joint fits of the lunar laser and planetary data. The new IAU precession (Lieske et al., 1977; Lieske, 1979) and nutation (Seidelmann et al., 1982) expressions have been used. A compatible integration of the lunar physical librations has also been made.

It is clear that the parameters which describe the geocentric distance of the moon will be very well determined from range data and have high internal precision. Of more interest for coordinate frames are the uncertainties in the orientation angles and rates of rotation with respect to inertial or terrestrial systems. The uncertainty in the orientation of both the lunar orbit plane and the ecliptic plane with respect to the equator of the earth is less than 0.01" (at least during the decade spanned by the observations). High sensitivity to the orientation of the ecliptic results from the lunar range data because the lunar orbit plane effectively precesses along the ecliptic.

The 18.6 yr period of precession is longer than the existing span of lunar laser data so that these orientations are improving rapidly as the data span increases. In addition to the orientation of the equator and two orbit planes we wish to know the relative error in the geocentric ecliptic longitudes of the moon and sun. A reasonable uncertainty for the differential longitude (during the past decade) is 0.003", being somewhat worse at the ends than in the center of the data span (1975). The sensitivity to the differential longitudes comes through two very strong solar perturbations (amplitudes of 3000 kms and 4000 kms) in the lunar distance. Thus the relative positions of the moon and sun are well known as seen from the earth. Since planetary ranging data to Mercury, Venus, and Mars determines their orbits well relative to the earth's orbit, they are also well connected to the lunar orbit and the earth's equator.

It has been argued that the lunar orbit and the earth's orbit about the sun are highly consistent in angular orientation, but what about rate errors? The integration of the equations of motion assumes an inertial coordinate frame, but the accuracy with which the range measurements can be related to the frame depends on the uncertainty in the mean motion (there are no solution parameters corresponding to orbital rates about the other two axes). For the moon the mean motion uncertainty is about 0.0007"/yr at the center of the data span (middle 1975), but at five years on either side it degrades to about 0.001"/yr. This growth of uncertainty results from an uncertainty in the lunar tidal acceleration of about 0.00015"/yr². The errors in the lunar ecliptic longitude grow nonlinearly as one extrapolates the motion outside of the span of data. In terms of its value for future UT1 determinations, the error of the new ephemeris will propagate with components of about 0.05 ms/yr and 0.005 ms/yr² from the center of the data span. At the time of the MERIT campaign this error would look mostly like an offset in UT1, but this can be reduced considerably with ephemerides produced closer to the beginning of the campaign and can be effectively eliminated with post-campaign analysis. The uncertainty in the inertial mean motion of the earth about the sun is 0.0002"/yr, being tightly determined by the excellent Viking range data from earth to Mars. The lunar and planetary ephemerides are very good representations of the inertial motions of the earth and moon during the past decade. Relating the inertial frame to a terrestrial frame requires knowledge of the precession constant which has an uncertainty of 0.0015"/yr (Fricke, 1977), of which 0.0006"/yr can project into declination. The consequences of this larger error have been explored by Williams and Melbourne (1981). If the accuracy of the inertial frame is to be preserved for the terrestrial longitude and UT1 systems, then the equation for Greenwich Mean Sidereal Time would need to allow for future improvements in the precession constant.

The new ephemerides are on a dynamical equinox so that the mean equator and mean ecliptic cross (at the dates J2000 or B1950.0) at the zero point for right ascension and ecliptic longitude. It is intended that the FK5 star catalogue will have a zero point close to (within several hundredths arcsecond) the dynamical equinox. Since we can align the zero point of our ephemerides with the dynamical equinox

an order of magnitude more accurately than we can align with a star catalogue, we have done so. My colleague E. M. Standish has located the dynamical equinox with an accuracy of at least a few milliarcseconds, and perhaps as good as 0.001". The conceptual simplicity of the dynamical equinox can be contrasted with previous attempts to align JPL ephemerides with the catalogue equinox of the FK4, which has the zero point of the right ascension system shifted about 0.5" (at B1950.0) from the dynamical equinox (Fricke, 1981). The modeling for the optical positions included shifts of each observational star catalogue from the FK4, corrections for equinox drift and the precession constant, plus systematic phase corrections for each planet. The zero point would shift slightly with each addition of new optical data. For ephemerides to be used with range data adopting the dynamical equinox is a welcome way to stabilize the zero points of the celestial right ascension and terrestrial longitude systems, it matches the (IAU sanctioned) FK5 equinox within the optical errors, but it is not strictly an IAU convention.

When one realizes that the lunar and planetary ephemerides are both accurate and can be used to achieve a nearly inertial celestial frame, it then becomes desirable to link with the frame of the other accurate, nearly inertial technique, very long baseline interferometry (VLBI). My colleague X X Newhall is attempting to do this using differential VLBI data which was recorded when the Viking Mars Orbiters and a quasar were close together in the sky. Preliminary indications are that this link can be achieved to better than 0.01", so that the VLBI quasar coordinate frame can be put on the dynamical equinox in the near future. If this is done the terrestrial longitude systems will line up to comparable accuracy.

Achieving a similarly accurate link with the optical frame is harder, but there is a possibility that the Hipparcos astrometry satellite and the Space Telescope can be used to connect optical positions of quasars with their radio counterparts toward the end of this decade (Kovalevsky and Preston, 1981, private communication).

Artificial satellite ranging by itself achieves neither an accurate inertial celestial frame, nor absolute zero point information on terrestrial longitudes (relative longitudes are well determined). As several observatories will soon be ranging both LAGEOS and the moon, it will soon be possible to directly align the artificial satellite (terrestrial longitude) coordinate system with the lunar laser system by comparing the site coordinates. If the LAGEOS data reduction programs were to also use the long-term stable UT1 values available from lunar laser ranging and VLBI, then the satellite orbit frame would automatically be aligned with the inertial celestial frame.

In summary, lunar and planetary ephemerides have been generated which result from joint data fits and integrations. The lunar orbit and the earth's orbit are oriented with accuracies better than 0.01" about two axes, and several times better about the third (ecliptic pole) axis. The zero point in right ascension is adjusted to a dynamical equinox, and the motions of the earth and moon have uncertainties within 0.001"/yr of their true inertial values during the past decade. It should be possible to connect the celestial frames of VLBI and the ephemeris and to tie together the terrestrial frames of satellite and

lunar ranging, so that the three modern space techniques would be aligned within 0.01" of one another. If this unification were to be made in the near future it would cause the minimum inconvenience since a concurrent introduction of the new IAU constants and definitions would also introduce shifts in the coordinate systems.

ACKNOWLEDGMENTS

The planetary work which I have described is a product of the efforts of E. M. Standish. The lunar laser data analysis was a joint effort between J. O. Dickey and myself. This paper presents the results of one phase of research carried out at the Jet Propulsion Laboratory, California Institute of Technology, under contract No. NAS 7-100, sponsored by the National Aeronautics and Space Administration.

REFERENCES

- Fricke, W., "Arguments in favor of a change in precession", *Astron. Astrophys.* 54, 363-366, 1977.
- Fricke, W., *Astron. Astrophys.*, in press, 1981.
- Lieske, J. H., T. Lederle, W. Fricke, and W. Morando, "Expressions for the precession quantities based upon the IAU (1976) system of astronomical constants", *Astron. Astrophys.* 58, 1-16, 1977.
- Lieske, J. H., "Precession matrix based on IAU (1976) system of astronomical constants", *Astron. Astrophys.* 73, 282-284, 1979.
- Seidelmann, P. K., V. K. Abalakin, H. Kinoshita, J. Kovalevsky, C. A. Murray, M. L. Smith, R. O. Vicente, J. G. Williams, Ya. S. Yatskiv, "1980 IAU theory of nutation, the final report of the IAU working group on nutation", *Celestial Mech.*, in press, 1982.
- Williams, J. G. and W. M. Melbourne, "Comments of the effect of adopting new precession and equinox corrections", proceedings of IAU colloquium 63, High-Precision Earth Rotation and Earth-Moon Dynamics: Lunar Distances and Related Observations, ed. O. Calame, Grasse, France, in press, 1981.